Boston University Theses & Dissertations

2022

Characterization of an activated aluminum slurry and design of an aluminum slurry-fueled field cooking system

BOSTON UNIVERSITY

COLLEGE OF ENGINEERING

Thesis

CHARACTERIZATION OF AN ACTIVATED ALUMINUM SLURRY AND DESIGN OF AN ALUMINUM SLURRY-FUELED FIELD COOKING SYSTEM

by

SAMUEL WALLACE BRUSH

B.S., United States Military Academy, 2020

Submitted in partial fulfillment of the

requirements for the degree of

Master of Science

2022

Approved by

First Reader

Emily Ryan, Ph.D.
Associate Professor of Mechanical Engineering
Associate Professor of Materials Science and Engineering

Second Reader

Sheryl Grace, Ph.D.
Associate Professor of Mechanical Engineering

Third Reader

Eric Morgan, Ph.D.
Technical Staff
MIT Lincoln Laboratory, Group 47 - Energy Systems

ACKNOWLEDGMENTS

First, I would like to thank Professor Ryan, Professor Grace, and Dr. Morgan for sitting on my thesis committee. Next, I would like to thank the Office of Naval Research for sponsoring my project. I would like to thank MIT Lincoln Laboratory Group 47 for giving me the opportunity to pursue a degree at Boston University.

Furthermore, I would like to extend my gratitude to all of the people who directly contributed to the completion of the thesis. I could not have done it without you. A big thanks goes out to Dave Scott and Andrew Volpe at TOIL for their tremendous help in fabrication and machining. I would like to thank Andrew Roley and James Macomber for helping me with Arduino and electronics. I would like to thank Jude Kelly for his help with the reactions testing. A tremendous thanks goes out to Elizabeth Dalli and Deborah Burdick for handling my countless part orders and release review requests. I would also like to thank my sister Trilby for her help in editing my thesis.

Furthermore, I would like to extend my sincerest gratitude to Professor Ryan whose mentoring and guidance has made this possible. I appreciate her dedication to good science and for keeping me focused on writing a successful thesis.

Additionally, I would like to thank Eric Morgan for all the guidance he has given me over the past two years. He has provided so much insight and help in steering me towards a good solution and keeping the end goal in sight.

Finally, I would like to thank my friends and family for their continual support. A special thanks goes to the 2020 USMA Fellows and BU Men’s Ultimate for their friendship and support over the past two years.

CHARACTERIZATION OF AN ACTIVATED ALUMINUM SLURRY AND DESIGN OF AN ALUMINUM SLURRY-FUELED FIELD COOKING SYSTEM

SAMUEL WALLACE BRUSH

ABSTRACT

Elemental aluminum is highly reactive with water but is normally coated with a layer of aluminum-oxide, which prevents any interaction between the aluminum and the water. A process was recently developed that removes the aluminum-oxide layer and enables the aluminum-water reaction to occur and produce heat and hydrogen. The resulting fuel is a promising technology in reducing the logistical burden of fueling remote locations, due to its high energy density and ability to generate large volumes of hydrogen. However, there are significant challenges in dispensing the solid fuel that must be overcome before the fuel could be used in field applications. One avenue to address this problem is to transform the solid aluminum fuel into a slurry by mixing ground aluminum fuel particles and mineral oil. The objective of this work is to improve and characterize the aluminum slurry fuel and demonstrate an application for the technology.

First, experiments were conducted to improve the rheological properties of the aluminum slurry and characterize the impact of slurry parameters on reaction behavior. A study was conducted to identify the optimal pumping composition of aluminum-mineral oil slurry. Reducing the aluminum particle size and the addition of 2% bentonite and 1% fumed silica to the slurry were found to have the greatest reduction in viscosity and settling of the aluminum slurry. Another study examined the impact of particle size, temperature, and water turbulence on the reaction time and hydrogen release of the

aluminum slurry. Analysis suggests that the reaction rate of the slurry is limited by the mobility of the aluminum in the mineral oil. The data from the reaction experimentation can be found in the supplemental materials.

Second, a prototype cooking system was developed to demonstrate an application for the aluminum slurry and to use the heat from the aluminum-water reaction. The system displayed the ability to dispense aluminum slurry in a controlled manner, maintain a flame using generated low-pressure hydrogen, and heat a body of water using the aluminum-water reaction.

TABLE OF CONTENTS

LIST OF TABLES

LIST OF FIGURES

LIST OF ABBREVIATIONS

Al .... Aluminum

$Al(OH)_3$ .... Aluminum Hydroxide

C .... Celsius

g .... Grams

H_2 .... Hydrogen Molecule

H_2O .... Dihydrogen Monoxide

JP-8 .... Jet Propulsion 8

l .... Liters

MJ .... Megajoule

MRE .... Meal Ready to Eat

RPM .... Revolutions Per Minute

s .... Seconds

SFC .... Single Fuel Concept

SLPM .... Standard Liters Per Minute

UGR .... Unitized Group Rations

US .... United States

W .... Watt

WT .... Weight

1. INTRODUCTION

1.1 Introduction to the Problem

One of the biggest challenges with supplying energy to remote sites is the ability to transport fuel. Historically, petroleum-based fuels have been the solution to meeting the energy demand due to their high energy density. The United States Army relies on Jet Propulsion 8 (JP-8), a diesel-based fuel, to meet their remote energy needs. This reliance on a single fuel type became the doctrine of single fuel concept (SFC) during the Vietnam War (Weir, 1996). The SFC sought to simplify logistics so every system, from electricity generators to aircraft, could be powered by a single fuel source, but this advantage came at the expense of flexibility. Today, a large and complex infrastructure exists to facilitate the SFC, diminishing the ability to supply systems that can leverage the advantages of new energy technologies and improve designs of existing platforms. Additionally, the lack of systems that do not use JP-8 prevents the United States Military, the largest governmental carbon emitter in the US, from defining a feasible path to reduce emissions (Belcher et al., 2020). Other energy storage mediums, such as batteries and hydrogen, have struggled to replace fossil fuels in remote applications due to their low energy density, reducing their ability to meet energy demand.

In 2014, a process was developed that transforms aluminum into a solid fuel that reacts with water and produces significant amounts of heat and hydrogen (Slocum). This activated aluminum fuel acts as a high-density hydrogen delivery vector and a heat source. Activated aluminum shows promise as a supplemental energy provider to remote locations because it possesses higher energy density than JP-8. Furthermore, activated aluminum fuel can be fabricated using locally sourced aluminum scrap, reducing the need to import fuel (Godart, 2019). Additionally, due to the structural strength of aluminum metal, aluminum could be used for packaging and converted into fuel at forward operating bases, decreasing the demand for dedicated fuel resupply. However, there are some challenges to overcome before activated aluminum could be integrated into wider applications, due to the constraints of solid fuel dispensing. In an attempt to solve these problems, previous projects have converted the aluminum into a slurry with mineral oil, but the resultant aluminum slurry is highly non-Newtonian leading to significant dispensing difficulty. Additionally, previous projects have been focused on using aluminum as a hydrogen vector, but applications of the heat from the reaction are relatively unexplored. In this thesis, I aim to develop a slurry composition suitable for pumping, characterize the effects of slurry parameters on reaction kinetics and hydrogen production, and create an aluminum slurry-powered cooking system that dispenses aluminum slurry in a controlled manner and uses the heat from the aluminum-water reaction.

1.2 Introduction to Aluminum and Aluminum Fuel

1.2.1 Aluminum Production

Aluminum is an abundant material that is produced in large quantities and used as a common structural material. There are two types of aluminum available on the market: primary and secondary. Primary aluminum is initially mined as bauxite ore before it is converted into aluminum metal. The conversion method from bauxite into aluminum requires two energy-intensive processes: the Bayer process and the Hall-Héroult process

(Choate and Green, 2003). These processes convert bauxite to aluminum metal and consume 78 GJ/ton Al (Choate, 2003). Over 67,000 tons of aluminum are produced annually with most of the production taking place in China (International, 2022). Secondary aluminum is aluminum that has been previously used and recycled. Secondary aluminum is not put through the Bayer and Hall-Héroult processes making the process of recycling aluminum a low-energy intensive process, as the aluminum only needs to be melted and have impurities removed (Choate, 2003).

1.2.2 Aluminum-Water Reaction

When elemental aluminum comes into contact with water, it exhibits an exothermic reaction. At standard temperature and pressure, the reaction produces heat, hydrogen, and aluminum-hydroxide, (Godart, 2019)

$$2\mathrm{Al(s)} + 3\mathrm{H_2O(l)} \rightarrow 3\mathrm{H_2(g)} + \mathrm{Al_2(OH)_3(s)} + \mathrm{Heat}, \left(\Delta G = -899\ \frac{\mathrm{kJ}}{\mathrm{mol}}\right) \quad (1.1)$$

The reaction produces 1.24 liters of hydrogen gas for every gram of aluminum consumed. The reaction rate is highly dependent on the temperature of the water and follows a mostly Arrhenius relationship. The products of the reaction differ when reacted in higher pressure and temperature environments as seen in Figure 1. Furthermore, the reaction is not limited by pressure even though the volume of the products is significantly greater than the volume of the reactants (Godart, 2019).

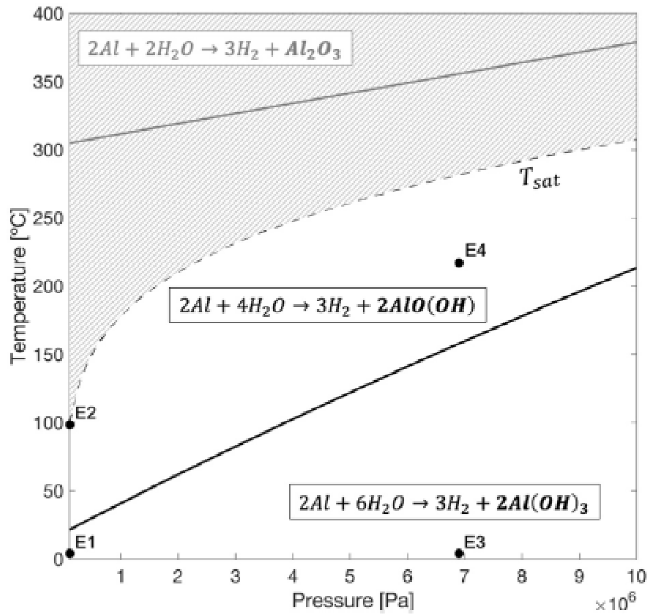

Figure 1: Aluminum-Water Reactions at Various Conditions (Godart, 2019)

1.2.3 Activated Aluminum Fuel Treatment Process

Aluminum metal normally reacts with air to form a strong oxide coating on the outside of the material, which renders the rest of the material from reaction. A treatment process was developed that removes the aluminum-oxide coating, allowing the aluminum-water reaction to occur. The treatment process starts with aluminum stock that is coldworked and broken into smaller pieces. The pieces are submerged in a bath of gallium-indium eutectic and heated to approximately 230℃ for an hour (Slocum, 2017). The gallium and indium diffuse into the aluminum, resulting in an alloy that is highly reactive with water, and becomes dull and brittle as seen in Figure 2. The resulting material contains 3-4 wt.% gallium-indium and can activate 90% of the aluminum to produce hydrogen in water (Slocum, 2017). The resulting transition enables elemental aluminum to exist at the surface of the material and react with water or other chemicals in the environment.

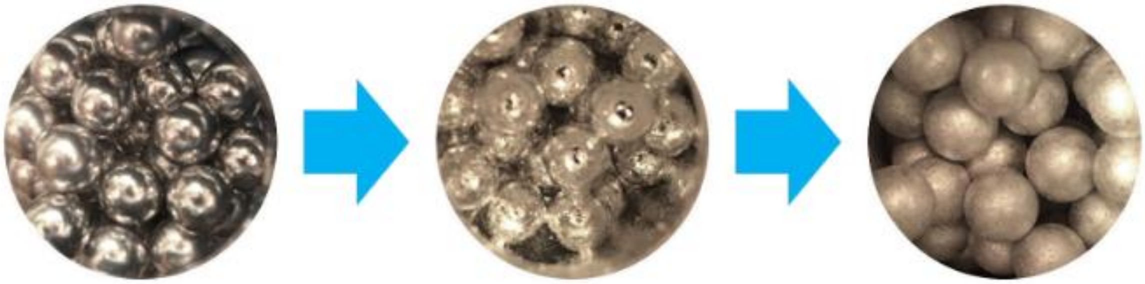

Figure 2: Activated Aluminum Treatment Process. Aluminum metal (left), Aluminum in Gallium/Indium Eutectic (center), Activated Aluminum (right). (Slocum, 2017)

1.2.4 Aluminum as a Fuel

Activated aluminum has a specific energy of 31 MJ/kg with 15.9 MJ/kg of the energy contained as hydrogen and 15.1 MJ/kg as low-quality heat. This fuel has an energy density of 83.7 MJ/l whereas diesel has an energy density of 43 MJ/l as seen in Figure 3 (Morgan, 2018).

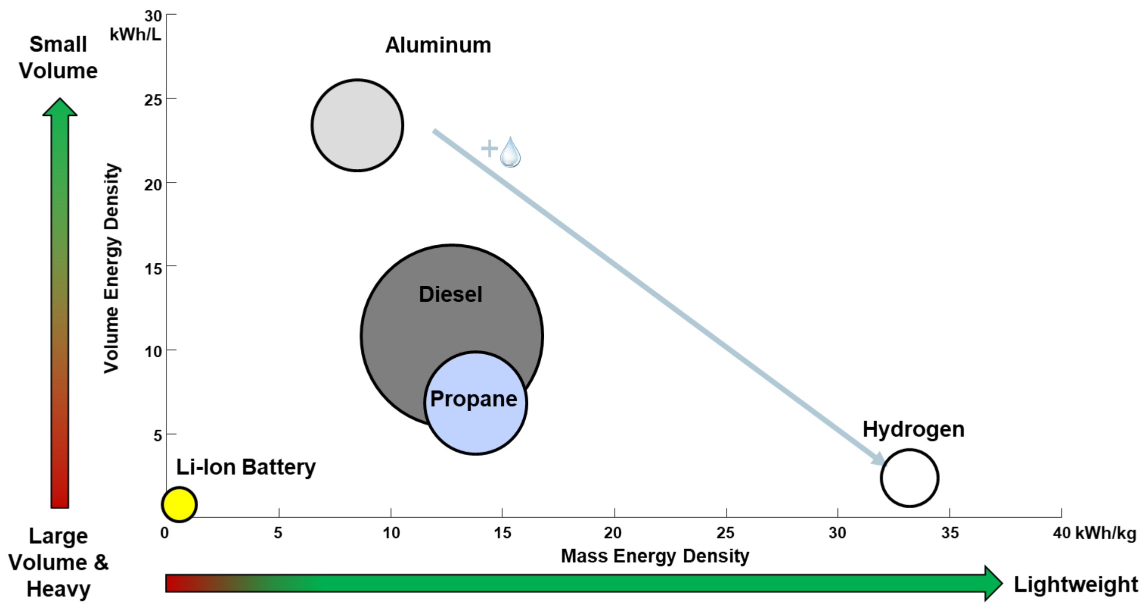

Figure 3: Energy Densities of Various Fuel Types (Morgan, 2018)

Due to the high energy density, activated aluminum fuel could translate well to use in space-constrained operations. Activated aluminum can deliver energy in a compact form, be scavenged on-site, and react with even poor-quality water and seawater, allowing hydrogen production at remote locations, even those without access to potable water. Additional aluminum could also be provided through aluminum packaging, which would reduce on-site waste. Furthermore, aluminum is a politically benign material, and the products of the aluminum-water reaction are safe, making it an unassuming fuel source for contested areas.

1.2.5 Current Activated Aluminum Reactors

There are two types of reactors that are currently used in activated aluminum systems: batch and continuous, as seen in Figure 4. In batch systems, activated aluminum and water are added to a reactor and the reaction progresses naturally without outside control. In continuous reactors, activated aluminum chips are continuously dispensed into a reactor, and the amount of aluminum reacted is dictated by the feed rate and the reactor conditions. In both systems, the aluminum reacts with the water in the reactor, and the hydrogen is removed from the reactor and directed to its end use, usually a fuel cell or storage vessel.

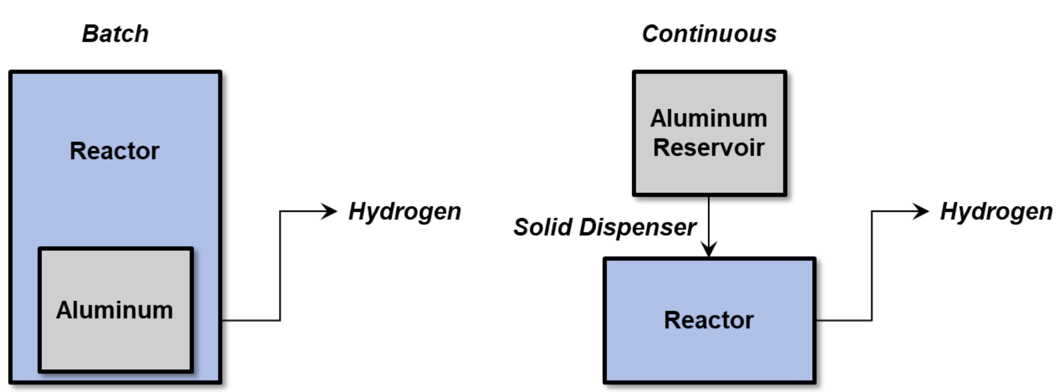

Figure 4: Current Aluminum Reactor Design Types

These systems have constraints due to the use of solid aluminum fuel. The fuel reservoir must be pressurized because the aluminum chip dispensing systems are unable to seal and hold pressure. Additionally, it is difficult to dispense solid fuel in a controlled manner due to pieces locking in place and jamming the system. These difficulties limit the ability to design compact and controlled systems.

1.2.6 Aluminum Fuel Slurry

The activated aluminum chips are ground into small particles and mixed with mineral oil to create a slurry (Fischman, 2020). Converting the aluminum into a non-homogeneous slurry addresses certain issues associated with dispensing solid activated aluminum chips. A sample of aluminum slurry can be seen in Figure 5. In this form, the aluminum flows as a high viscosity non-Newtonian fluid and is more easily dispensed.

Figure 5: Activated Aluminum Chips (left) and Slurry (right)

Aluminum fuel slurry has advantages over chips that make it a better fuel type. The aluminum slurry can be pumped, removing the need to pressurize the storage reservoir and reduces dispensing uncertainty and permits micro-dosing of fluid. The reaction kinetics of the slurry can be finetuned by using different additives and modifying the slurry properties. However, aluminum fuel slurry is still in an early stage of development and has some difficulties that must be addressed before it is used as the main fuel form in future systems. The slurry tends to jam in pipe restrictions and has a high viscosity (Fischman, 2020). Improving the rheological characteristics of the slurry would make it easier to dispense. While the reaction behavior of aluminum fuel chips is well characterized, the reaction behavior of the aluminum slurry is not as understood. Having information about reaction time and energy release profiles will help to improve systems that use aluminum fuel slurry.

1.3 Research Goals

The purpose of this thesis is to investigate the effects of material composition on activated aluminum slurry rheology and pump capability, evaluate the reaction kinetics of activated aluminum slurry, and design a cooking system powered by activated aluminum slurry. First, develop a slurry composition suitable for transportability at high aluminum content. Second, pump designs were evaluated to determine which types would be suitable for transporting the aluminum slurry. Third, activated aluminum slurry was tested to determine how reaction temperature, particle size, and water turbulence affected the reaction progression. Fourth, a prototyping effort was conducted to develop a 500 W cooking system that could controllably dispense aluminum slurry, heat a body of water, contain the generated hydrogen, and maintain a hydrogen flame. Finally, the results of the effort were summarized, and potential future research efforts were described.

2. REVIEW OF LITERATURE

2.1 Review of Non-Newtonian Fluids and Slurry Rheology

There are two classifications for fluids and their viscosities: Newtonian and non-Newtonian. The difference in the classification of the fluids is determined by how the fluids respond to various amounts of shear. Newtonian fluids have a linear relationship between the stress and the shear rate (Chhabra, 2010). Non-Newtonian fluids are fluids that follow a non-proportional relationship between stress and shear rate. There are three methods in which a fluid displays non-Newtonian behavior: time-dependent fluid properties, a non-linear relationship between stress and shear rate, or solid behavior below a certain shear stress threshold (Chhabra, 2010). A difference in the behavior of non-Newtonian fluids in response to shear can be seen in Figure 6.

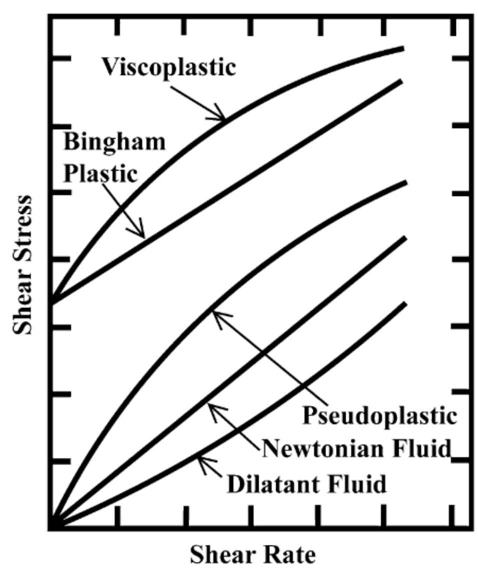

Figure 6: Flow Curves for Various Non-Newtonian Fluid Types (Chhabra, 2010)

These behaviors make it harder to transport the fluids reliably and consistently due to their non-regular behavior. The more the characteristics of a fluid deviate from traditional Newtonian behavior, the harder it is to dispense them (Chhabra, 2010). There are a wide variety of fluids that exhibit non-Newtonian behavior. Some common non-Newtonian fluids are peanut butter, ketchup, and cement, each of which come with specific pumping challenges.

2.2 Review of Aluminum Slurry Rheology

Most activated aluminum research has focused on using chips of solid aluminum as fuel (Godart, 2019). Activated aluminum is brittle and can be ground into fine particles to increase the dispensing ability of the fuel, but these fine particles can pose inhalation and explosive risks. It was discovered that the activated aluminum particles could be mixed with mineral oil to transform the fuel into a dilatant non-Newtonian fluid (Fischman, 2020). The process for making activated aluminum slurry can be seen in Figure 7. Mineral oil is a suitable carrier fluid for activated aluminum because it does not react with the aluminum, prevents contact with air, and does not experience off-gassing when heated (Fischman, 2020). These characteristics are ideal when trying to store and use activated aluminum because it prevents deterioration of the fuel and does not affect the chemistry of the reaction. Mineral oil also has a low vapor pressure meaning that it will not produce vapors that could potentially foul fuel cells or other systems that use the hydrogen from the reaction (Fischman, 2020).

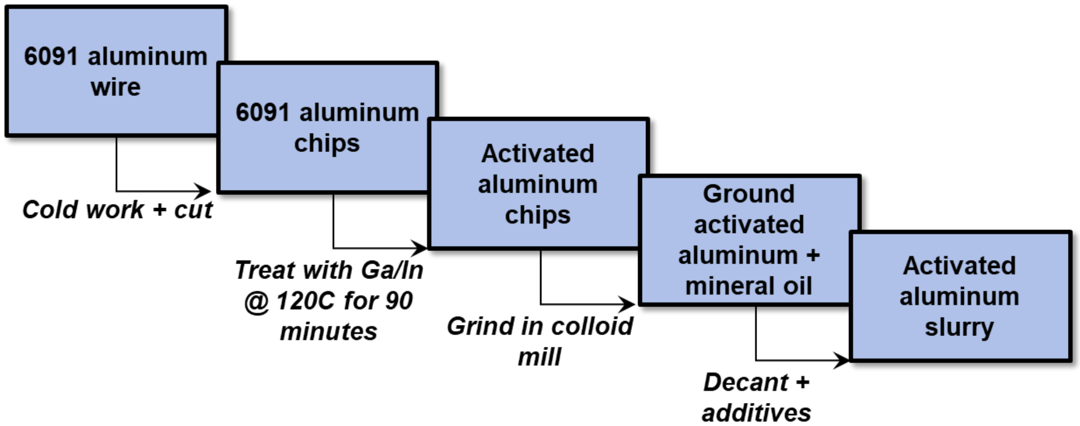

Figure 7: Activated Aluminum Slurry Fabrication Process

Creating a slurry lets the activated aluminum be transported as a fluid, but there are a few problems with the fuel form. The insolubility of the mineral oil in water results in a layer of oil that prevents the aluminum from contacting the water and reacting (Fischman, 2020). The resulting layer can either be broken by the aluminum particles naturally passing through less dense oil layer or through mechanical disturbance of the oil layer as seen in Figure 8**.**

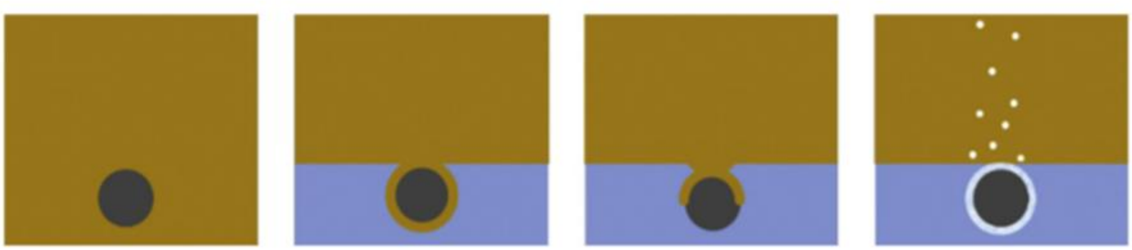

Figure 8: Process of Aluminum Slurry Reacting with Water. From Left to Right: Aluminum Grain in Oil, Aluminum Falls Through Oil, Aluminum Contacts Water, Hydrogen Generation Begins (Fischman, 2020).

Activated aluminum particles suspended in mineral oil tend to settle due to the difference in density between the aluminum and mineral oil resulting in a lack of homogeneity of the solution (Fischman, 2020). This separation results in non-uniform shear properties which make it more difficult to transport. When the particles settle, the layer of oil between particles thins to a point where there is not enough carrier fluid to prevent contact of the particles (Feyes, 2022). The particles lock and are unable to slide past each other, which results in a sharp increase in viscosity and a decreased ability to flow (Feyes, 2022). Additives have been found to decrease the settling and thicken the fluid, which increases the homogeneity of the fluid (Fischman, 2022). One example of an additive is Fumed silica which prevents settling by building a protective layer around the aluminum, preventing the particles from clumping together (Fischman, 2022). Other additives have been tested, but it is an ongoing field of study to determine which ones are most effective at improving aluminum slurry transportability.

Another issue with pumping slurries is that they are prone to jamming and experience sharp pressure drops through pumping systems. The main factors that affect the flow of the slurry are particle size, particle loading, the interaction between the particles and carrier fluid, pipe roughness, and flow velocity (Vlasak, 2011). At low velocities with large particles, the effects of settling in the bed of the pipes is the dominant contributor to pressure drop (Kaushal, 2005). With finer particles, the pressure drop is driven by frictional losses that increase with the velocity (Kaushal, 2005). For all slurries, the frictional losses increase when the concentration of suspended particles increases, and the diameter of the pipe decreases (Vlasak, 2011). The presence of bends or restrictions in the pipes correspond with sharp increases in pressure and can result in a buildup of particles that can prevent flow (Feyes, 2022). Restrictions in the fluid path can lead to the carrier fluid separating from the particles, causing clumping. This issue was observed in previous experiments that pumped activated aluminum slurry with a syringe pump (Fischman, 2022).

There are a multitude of pump designs that can be used for pumping slurries. For slurries, pumps that cause low amounts of shear on the fluids are desirable because the impact of non-Newtonian fluid behavior is reduced (Vlasak, 2011). The fluid becomes highly resistant to flow as the shearing increases in the fluid. In the concrete industry, the most common types of pumps are double piston pumps and screw pumps (Feyes, 2022). These pumps are used because they are characterized by low fluid shear and the ability to handle high solid loading. Furthermore, double piston pumps constantly agitate the mixture in the hopper to prevent settling of the slurry.

2.3 Review of other Water Reactive Metal Slurries

A common property of certain metals is the ability to react with water to produce hydrogen. This reaction occurs because the metal atoms are positively charged and form bonds with hydroxide ions from water, with the leftover hydrogen atoms forming hydrogen gas (Züttel, 2004). A commonly used metal for heat and hydrogen generation is magnesium. Magnesium pellets are used as the primary heat source for military ration heaters and other water activated cooking heaters (Barrett, 2010). A magnesium hydride slurry was developed by Fraunhofer IFAM that produces heat and hydrogen using the reaction of magnesium in water (2013). The magnesium hydride slurry paste has a reported energy density that is ten times greater than lithium-ion batteries after energy conversion losses (Fraunhofer, 2013). The magnesium hydride slurry is similar to the activated aluminum slurry, but has a lower energy density due to aluminum-water reaction being more energetic than the magnesium-water reaction.

3. SLURRY CHARACTERIZATION EXPERIMENTATION

3.1 Introduction to Slurry Experiments

The first goal of the thesis is to develop and characterize an aluminum-fuel slurry. The first part of this chapter will cover how the aluminum slurry was created, the process of determining an optimal slurry composition, and the design of aluminum-slurry pumps and dispensing methods. Dispensing the aluminum-fuel as a liquid slurry fuel should be easier to dispense than solid fuel, but due to the highly non-Newtonian behavior of the slurry there were challenges that do not occur with Newtonian fluids.

The second part of this chapter will cover the methods of testing the reaction kinetics of the aluminum slurry. Knowledge on the impact of fuel parameters informs decisions on reactor and control system design. Prior testing on aluminum reaction kinetics was mostly limited to testing aluminum chips without the presence of mineral oil. The goal is to determine how changes in the slurry and the reactor conditions impact the reaction, and which factors are most important.

3.2 Slurry Creation Process

The aluminum slurry is created from aluminum fuel chips and mineral oil using a Bematek Model CBT-50-PB-1½ colloid mill seen in Figure 9. The mill cycles mineral oil through the head of the colloid mill. The head of the colloid mill is set to 30 RPM and set to a head space of 1 mm. Chips of aluminum fuel weighing 0.15 grams are slowly added to the hopper and broken down while passing through the head of the colloid mill. Once the desired amount of aluminum is added, the head space in the colloid mill is slowly reduced to break the aluminum into smaller particles. The head space is decreased until the flow rate of the mineral oil-aluminum mixture is significantly reduced, and the desired particle size is reached.

Figure 9: Colloid Mill Used for Producing Aluminum Slurry

The aluminum-oil mixture is drained from the colloid mill and set to decant overnight. The aluminum particles settle at the bottom of the oil enabling the excess oil to be poured out, leaving a mixture of approximately 50 wt.% aluminum and 50 wt.% mineral oil. Additional mineral oil can be added or decanted to adjust the ratio of aluminum to mineral oil. Bentonite and/or fumed silica is added to reduce separation of the activated aluminum slurry and decrease the viscosity. Samples from each part of the slurry creation process can be seen in Figure 10.

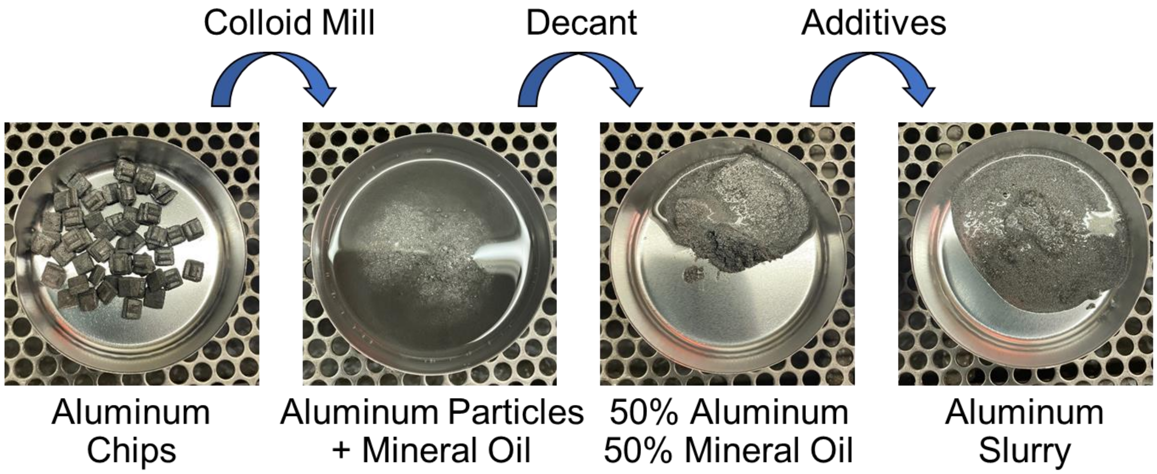

Figure 10: Slurry Preparation Process. The mixture settles into layers of aluminum particles and oil, the excess oil is removed, and additives are added.

3.3 Slurry Composition Experiment

The goal of the slurry composition testing was to examine the effects of additives, oil content, and particle size on the rheological behavior of the slurry, to develop a slurry composition that would perform the best in the pumping experiments. The best configuration would have high mobility and aluminum content. Slurries with various compositions were tested to find the mixture that had the best mobility with the highest aluminum content. Bentonite content, fumed silica content, and particle size were tested for their impact on slurry viscosity and settling reduction. The parameters that were tested can be seen in Table 1.

Table 1: Test Matrix for Slurry Composition Experiment

Tested Parameters				**Tests**
Particle Size (mean diameter µm)	Oil Content (wt.%)	Bentonite (wt.%)	Fumed Silica (wt.%)	Falling Film
Large (700)	40	0	0	Shock
Small (300)	50	2	1	Pour
	60	4	2	
		6	4	

To evaluate each of the samples, 10 grams of aluminum slurry is placed into weigh dishes and observed under different disturbance conditions. For the falling film test, the slurry is set to one side of the weigh dish and is put at a 75-degree incidence angle to see how fast it travels down to the bottom of the dish. For the shock test, the slurry is clumped together in the center third of the dish and the dish is shaken until a film of aluminum slurry covers the surface of the dish. For the pour test, the aluminum slurry is clumped in the side of the dish and is poured into another weigh dish. The properties of the various slurries are qualitatively observed to identify which samples had the highest mobility. The composition with the highest mobility would be used for the later pumping experimentation and in the cooking system prototype.

3.4 Slurry Composition Results

Mixtures with higher aluminum content were more resistant to flow. When the concentration of aluminum exceeded 60 wt.%, the slurries became highly resistant to flow and had a drier consistency as seen in Figure 11. This behavior is less desirable for pumping applications because the high concentration aluminum slurry is likely unable to self-prime the pump. Mixtures with 40-50 wt.% content aluminum had a significant decrease to the viscosity of the slurry.

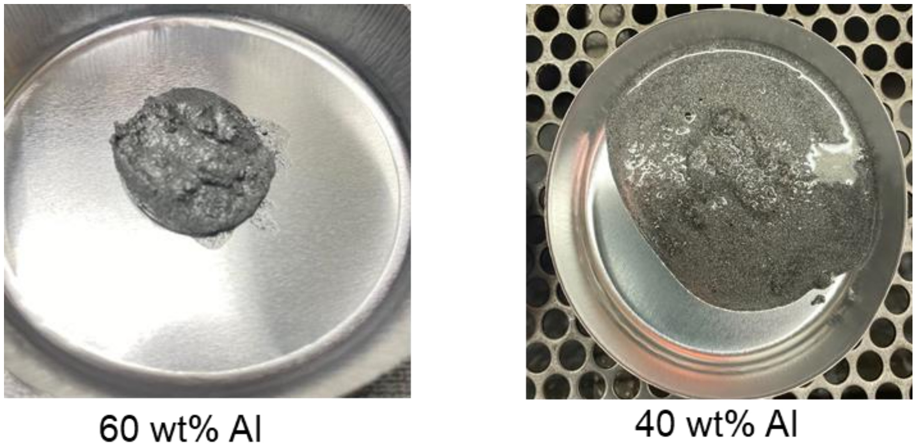

Figure 11: Effect of Aluminum Concentration on Slurry

It was found that reducing the particle size led to a significant increase in the mobility of the slurry. Two samples of the coarse and fine slurry can be seen in Figure 12. When the aluminum particles are larger, the slurry behaves like wet gravel, while a slurry with smaller particles behaves like a thick fluid. The slurry with smaller particles likely has increased mobility because it is easier for the particles to separate after they come into contact with other particles.

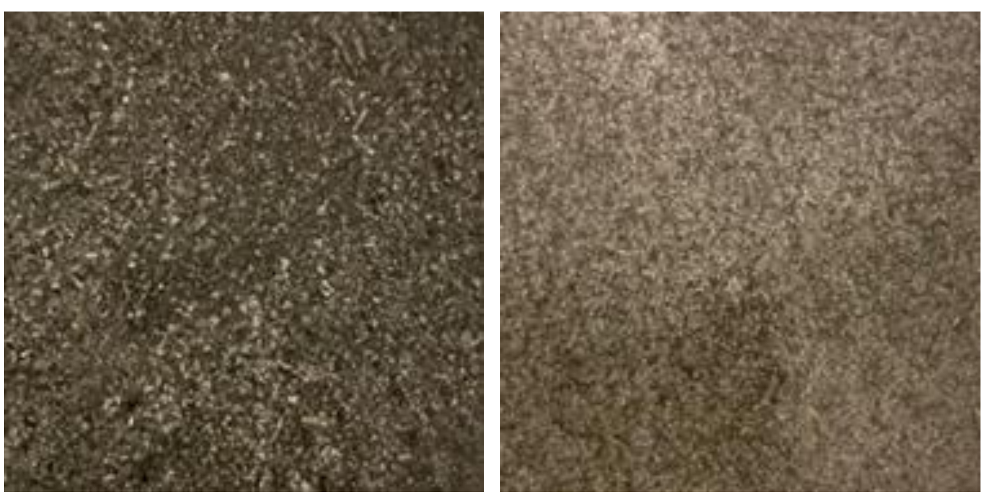

Figure 12: Coarse (700 µm) (left) and Fine (300 µm) (right) Aluminum Slurry

It was discovered that small additions of bentonite and fumed silica improved the rheological characteristics of the slurry. The addition of 2 wt.% bentonite into the mixture significantly decreased the viscosity of the slurry while additions above 4 wt.% bentonite corresponded with an increase in viscosity of the fluid. The addition of 1 wt.% fumed silica to a slurry with 2 wt.% bentonite was found to increase the homogeneity of the slurry and prevent settling. If too much fumed silica was added, the mixture would dry up and the viscosity increased to a point where the slurry would not quickly respond to disturbances.

It was found that decreasing the concentration of aluminum was most effective at increasing the ability to pump the slurry, followed by reducing the aluminum particle size, addition of bentonite, and addition of fumed silica. The optimal slurry composition used for the pumping tests contained 50 wt.% aluminum, 2 wt.% bentonite, and 1 wt.% fumed silica with aluminum particles with a mean diameter of 300 μm.

3.5 Slurry Pump Evaluation

The goal of the pump evaluation was to select a pump to use for the cooking system prototype described in Chapter 4. The pump would need to be able to consistently dispense 15 mL of activated aluminum slurry per minute to generate the desired power. A review of different pumping technologies was conducted to select a pump type to use for the project. The most important characteristics for selecting a slurry pump for the project are simple design, low fluid shear, ability to hold pressure, and ability to handle fluids with high solid content. The results of the survey can be found in Figure 13. The most promising pump types are screw pumps, progressive cavity pumps, and piston pumps. These pumps are commonly used for transporting slurries as they impart low shear on the non-Newtonian fluids. While the progressive cavity and piston pumps show promise for future work and would likely be more effective at pumping aluminum slurry in pressurized applications, the screw pump was chosen due to the simplicity of the design and low shear on the fluid. A peristaltic pump was also tested because of its ability to smoothly dispense fluids at low feed rates.

Pump	Fluid Shear	Complexity	Solid Loading	Flow Consistency	Pressure Handling
Progressive Cavity	Low	Med	Good, some ware on stator	Good, depending on size	Good, some slipping may occur, add more chambers
Screw	Low	Low	Good	Very Smooth	Dependent on Viscosity
Lobe/Gear	Low/Med	Low/Med	Good/Bad	Good, depending on size	Okay/Good
Flexible Impeller	Low	Med	Med, some impeller degradation	Very Smooth	Okay
Centrifugal	Med	Low	Bad	Very Smooth	Bad
Peristaltic	High	Low	Bad	Very smooth for low solid fluids	Okay
Piston	Low	Med	Okay	Highly Periodic	Good
Diaphragm	Low	High	Good	Highly Periodic	Good

Figure 13: Evaluation Matrix of Various Pumping Technologies

The screw pump was designed in SolidWorks and printed using a Stratasys J750 3D printer. The peristaltic pump was a MasterFlex L/S Model 77252-62 and used size 15 MasterFlex tubing. The pumps can be seen in Figure 14. The pumps were tested for ability to transport slurry and the frequency of jamming. The pumps pulled aluminum slurry from a reservoir and dispensed the aluminum. The pumps were operated until a failure occurred and issues with the pumping were identified.

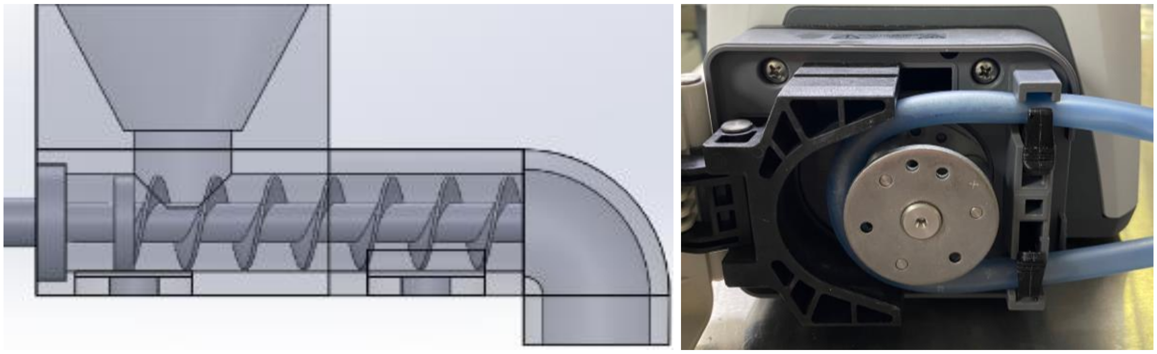

Figure 14: Pumps Tested: Screw Pump (left) and Peristaltic Pump (Right)

3.6 Slurry Pumping Results

The first pump that was tested was the peristaltic pump. This pump successfully self-primed the aluminum slurry from the reservoir and passed the aluminum through the rollers It was discovered that when there were any restrictions in the tube after the pump head, the aluminum slurry would get compressed and form a solid mass of aluminum. The compression removed the mineral oil from the slurry, leaving only solid aluminum particles. The jam would propagate back up the tubing as more slurry was fed through the pump head. This behavior is consistent with testing done with syringe pumps by Fischman in prior experiments, where the reduction in the cross-section of the channel forced aluminum particles closer together and the pump jammed (2020).

The second pump tested was the screw pump. The screw pump was found to be effective at pumping the aluminum slurry as it did not impart significant shear on the fluid. However, it was prone to jamming due to aluminum particles getting stuck between the rotor and stator. Decreasing the average aluminum particle size of the slurry reduced the frequency of jamming. Aluminum slurry occasionally built up at the pump outlet and reduced the flow rate of aluminum entering the reactor. Reducing the feed rate of the pump to enable time for the slurry to clear from the outlet reduced the buildup. The screw pump was the most effective design between the two pumps as it was able to dispense aluminum slurry more reliably and was less prone to jamming.

3.7 Slurry Reaction Testing

3.7.1 Introduction to Slurry Reaction Testing

Slurry reaction testing was conducted in an EasyMax chemical synthesis reactor. The goal of the testing is to determine the effect of different slurry parameters and environmental conditions on reaction progression. The effects of aluminum particle size, reaction temperature, and stirrer speed were tested for their impact on the variables of peak hydrogen release rate, total hydrogen release, and reaction completion time. The test matrix can be seen below in Table 2, which details all the parameters that were tested.

Table 2: Slurry Reaction Kinetics Test Matrix

Tested Parameters			Dependent Variables
Particle Size (mean diameter (µm))	Stirrer Speed (RPM)	Temperature (°C)	H2 Produced (l/gAl)
.15 g Chips	100	30	Peak H2 Production Rate (SLPM/gAl)
Large (700)	200	50	Reaction Time (s)
Medium (300)	300	70	
Small (100)		90	

Four different fuel types were tested including aluminum chips and three particle size slurries with mean particle diameters of 700, 300, and 100 µm as seen in Figure 15. It was predicted that as the aluminum mean particle diameter decreases, the complete reaction time increases, and the peak reaction rate would decrease due to the increased difficulty for the smaller aluminum particles to separate from the oil. It was expected that changes in the particle size would have no impact on the total amount of hydrogen evolved.

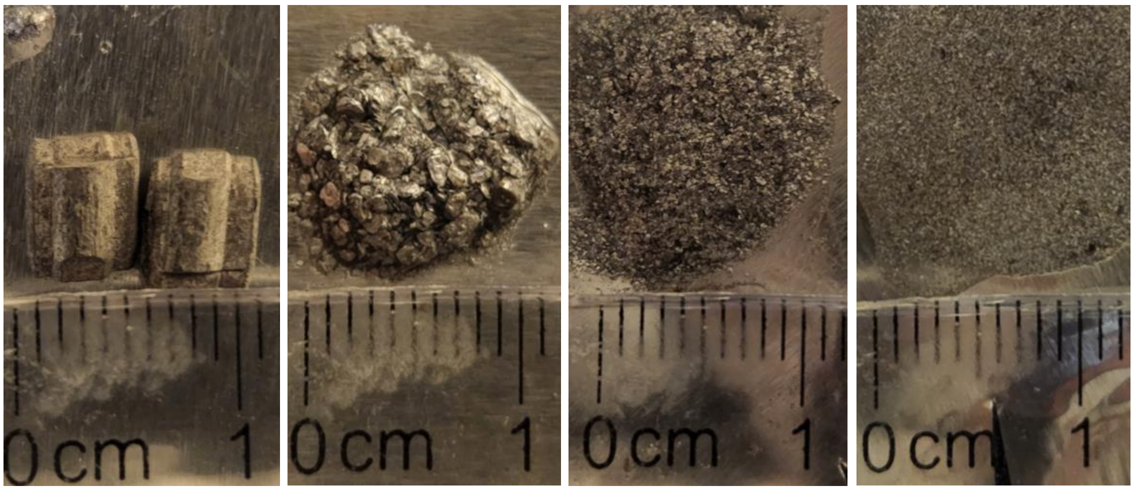

Figure 15: Particle Size Samples. Chips (Left), Large (Center-Left), Medium (Center-Right), Small (Right)

A range of reaction temperatures were conducted to evaluate how the reaction varied across typical operating temperatures. The temperatures from 30 to 90℃ were tested because most designed systems react the aluminum in this temperature range. The reaction rate is expected to significantly increase as the temperature increases. Various stir speeds were tested to evaluate the effect of turbulence on the reaction. Higher stir speeds correlate with higher water turbulence in the reactor. The EasyMax requires some degree of stirring to ensure sufficient mixing of the water, so the reactor has a more uniform temperature. Increasing the stir rate is expected to decrease the reaction time because the aluminum will be able to separate from the oil faster.

3.7.2 Experimental Setup

An EasyMax 102 semi-automated chemical synthesis reactor is used to conduct the experiment. The EasyMax reactor can stir and adjust the temperature of a liquid housed inside the reactor while taking measurements. The system is fitted with a hermetically sealed magnetic stirrer, heater, temperature sensor, Alicat mass flow controller, and PH probe as seen in Figure 16. The Alicat mass flow controller was used to measure the hydrogen generated from the reaction. Testing procedures were programmed in the iControl software application.

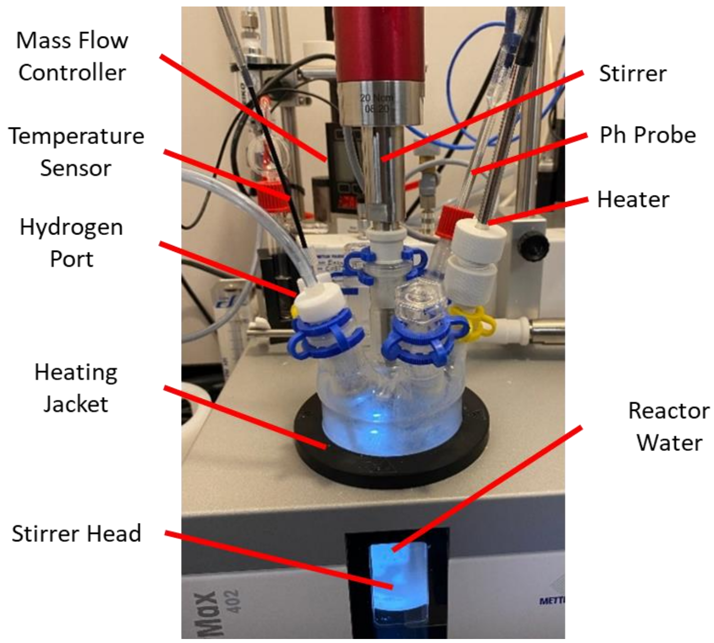

Figure 16: Easy Max Reactor with Measuring Equipment

The reactor is filled with 400 mL of 2 ppb Deionized water and the air was purged with nitrogen. The Easymax holds the reactor isothermal and stirs the liquid at a constant rpm. The water is held at 50°C, stirred at 200 rpm, and the medium (300 µm) particle size slurry is used except when testing those parameters. The slurry contained aluminum and light viscosity mineral oil with a concentration of 52.6% aluminum and contained no additives. Each test would have five subsequent slurry additions of approximately 0.6 g aluminum.

3.7.3 Reaction Testing Procedure

The experiment is started after the reactor equipment is setup, the 400 mL of water is added, and the air is purged with nitrogen. The EasyMax begins collecting PH, temperature, hydrogen flow, and heat generation data. The water is heated to the desired reaction temperature and the stirrer is set to the desired rpm. The system evaluates the heat capacity of the reactor. Once complete, the first sample of slurry is weighed and manually dropped into the reactor. The slurry reacts with the water and the reaction progresses until completion or until 10 minutes after the fuel was added, whichever time was longer. The EasyMax works to maintain the temperature of the water during the reaction time. Five fuel samples are added for each parameter for the particle size, temperature, and spin speed experiments. After the collection is completed, the data is normalized to the mass of added aluminum and adjusted to correct errors. Samples are removed from the dataset that had no significant hydrogen generation which is indicative of a sampling error or a broken seal. The remaining samples and are averaged together to create an average hydrogen generation profile for the corresponding particle size, temperature, and spin speed. The normalized hydrogen release data can be found in the supplementary materials.

3.8 Slurry Reaction Test Results

3.8.1 Effect of Temperature on Reaction Kinetics

Prior testing with aluminum chips has shown that the aluminum reaction rate is exponentially dependent on the temperature of the water and this behavior was observed with the aluminum slurry reaction. The peak reaction rate is exponentially related to the temperature as seen in Figure 17. However, the total reaction time is not exponentially related to the inverse of temperature as seen in Table 3. This difference is likely due to the transport of aluminum particles through the mineral oil limits the ability for the reaction to completely progress.

Table 3: Effect of Temperature on Average Hydrogen Production

Temperature (°C)	Reaction Time (s)	Peak H2 Production Rate (SLPM/gAl)	H2 Produced (L/gAl)
30	1310	0.047	0.156
50	1550	0.222	0.703
70	680	0.785	1.12
90	580	6.08	1.15

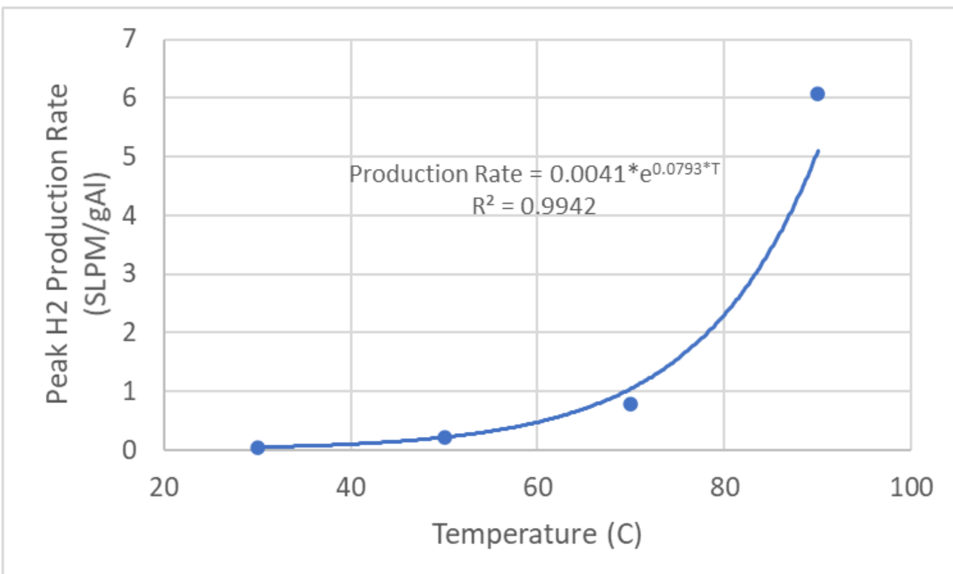

Figure 17: Peak Production Rate as a Function of Temperature

The water temperature also has a significant effect on the amount of hydrogen produced as seen in

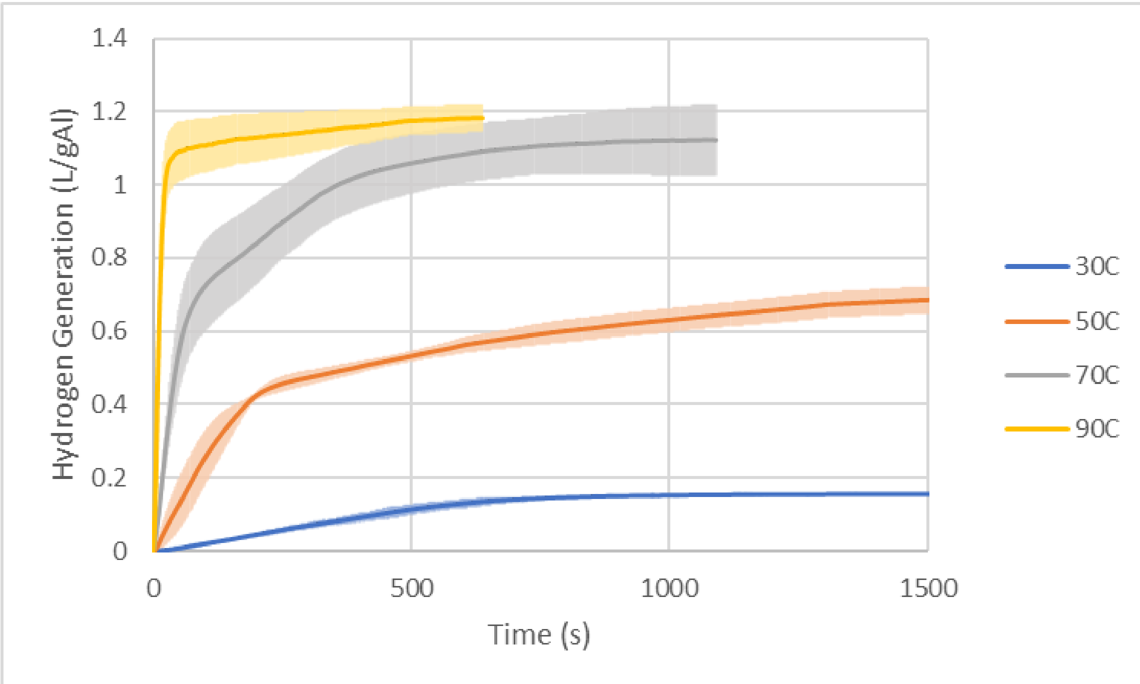

Figure 18. At higher temperatures, the amount of hydrogen released approaches the theoretical production rate of 1.24 liters of hydrogen per gram of aluminum. At lower temperatures, the reaction occurs at a lower rate and reaction efficiency decreases as less of the aluminum reacts with the water. For designing systems that use the activated aluminum slurry, operating in higher temperature regimes would produce higher energy output due to increased aluminum reaction efficiency.

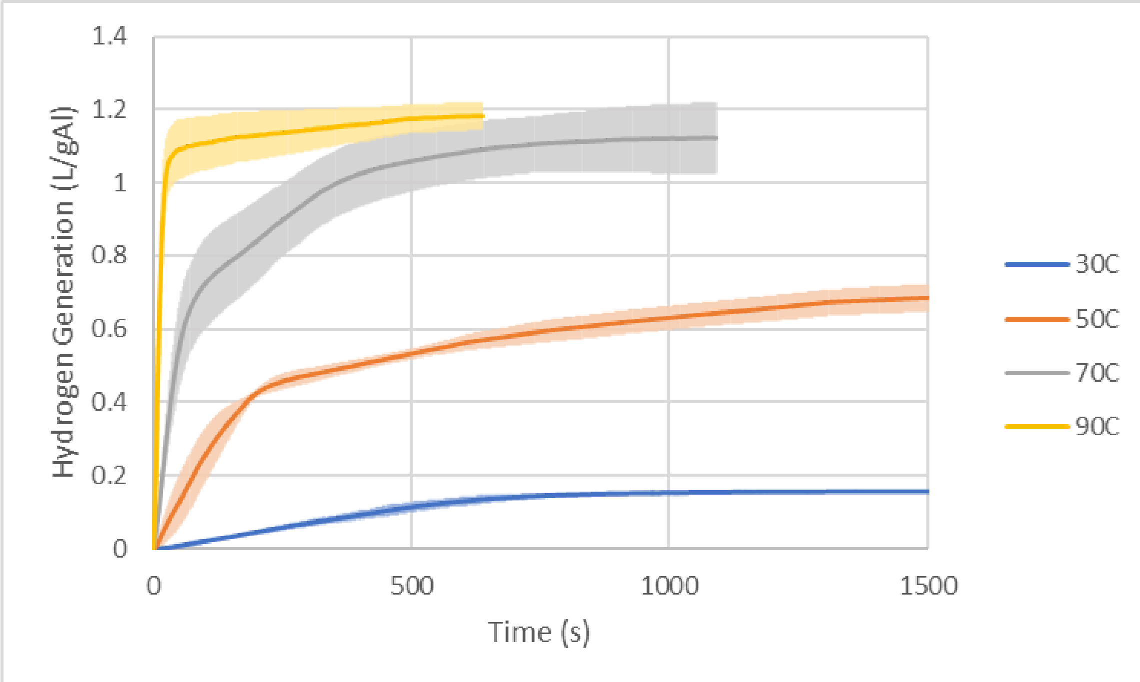

Figure 18: Integrated Hydrogen Production of Various Temperatures. The lines represent the average integrated hydrogen generation profile of each test. The shaded regions depict the standard deviation of the test samples.

3.8.2 Effect of Particle Size on Reaction Kinetics

The size of the aluminum particles had a significant impact on the reaction time and peak hydrogen production rate. The effects of the particle size on the reaction can be seen in Table 4. The time for the reaction to reach completion increased as the aluminum particle size decreased. This effect was likely caused by the increased difficulty for smaller particles to overcome the effects of surface tension and interact with the water. The same phenomenon is likely responsible for the peak production rate. The peak hydrogen production rate occurred later as particle size decreases as seen in Figure 19.

Table 4: Effect of Particle Size on Average Hydrogen Production

Particle Size (mean diameter (μm))	Reaction Time (s)	Peak H2 Production Rate (SLPM/gAl)	H2 Produced (L/gAl)
.15 g Chips	220	1.04	0.988

Large (700)	560	0.439	0.767
Medium (300)	1550	0.222	0.703
Small (100)	1690	0.167	0.768

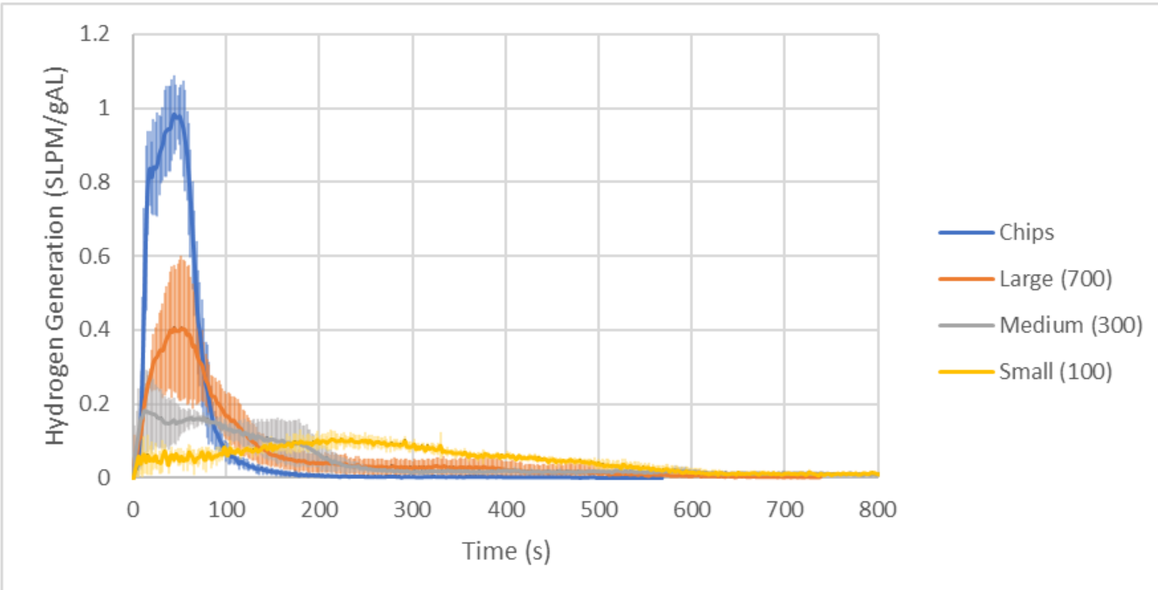

Figure 19: Hydrogen Production Profile of Various Particle Sizes. The lines represent the average hydrogen generation profile of each test. The shaded regions depict the standard deviation of the test samples.

The particle size of the slurry fuel did not have a significant effect on the total amount of hydrogen produced for each of the slurry cases as seen in Figure 20. However, the chips produced significantly more hydrogen than each of the slurries. It is possible that the high reaction rate of the chips caused some local heating that the EasyMax could not control leading to a higher reaction efficiency as discussed in the previous section, increasing the total hydrogen production.

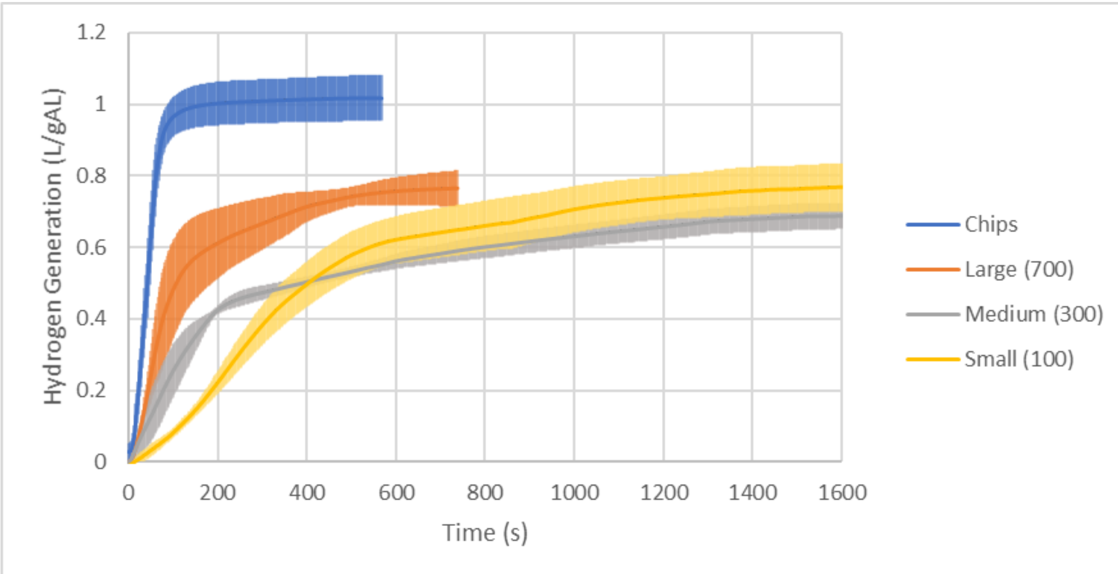

Figure 20: Integrated Hydrogen Production of Various Particle Sizes. The lines represent the average integrated hydrogen generation profile of each test. The shaded regions depict the standard deviation of the test samples.

3.8.3 Effect of Spin Speed on Reaction Kinetics

As the spin speed increased, the reaction time significantly decreased as seen in Table 5. The turbulence at higher stir speeds likely caused aluminum particles to separate from the oil faster and react with the water as seen in Figure 21. However, the effect on the peak hydrogen production rate was minimal when compared to particle size or temperature. This result suggests that the mass transport limitations hinder the total reaction progression, but the temperature-based reaction kinetics drive the peak reaction rate.

Table 5: Effect of Stir Speed on Average Hydrogen Production

Spin Speed	Reaction Time (s)	Peak H2 Production Rate (SLPM/gAl)	H2 Produced (L/gAl)
100 RPM	2270	0.166	0.852
200 RPM	1550	0.222	0.703
300 RPM	590	0.255	0.813

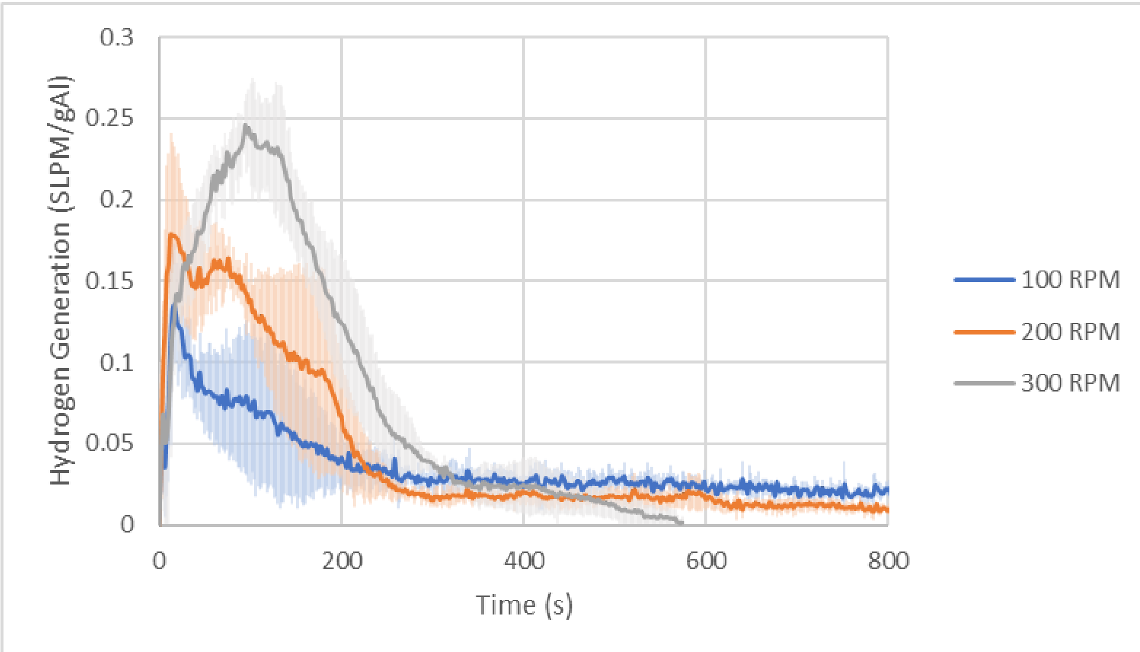

Figure 21: Hydrogen Production Profile of Various Stir Speeds. The lines represent the average hydrogen generation profile of each test. The shaded regions depict the standard deviation of the test samples.

The samples produced a similar amount of hydrogen initially, but the hydrogen production slowed for the slower stir speeds as seen in Figure 22. The aluminum slurry floats on the surface of the water, so the turbulence caused by the higher stir speeds likely disturbed the slurry faster and allowed the aluminum to contact the water. Stirring the water leads to faster reactions and would be more beneficial as a thicker layer of oil builds up at the top of the reactor.

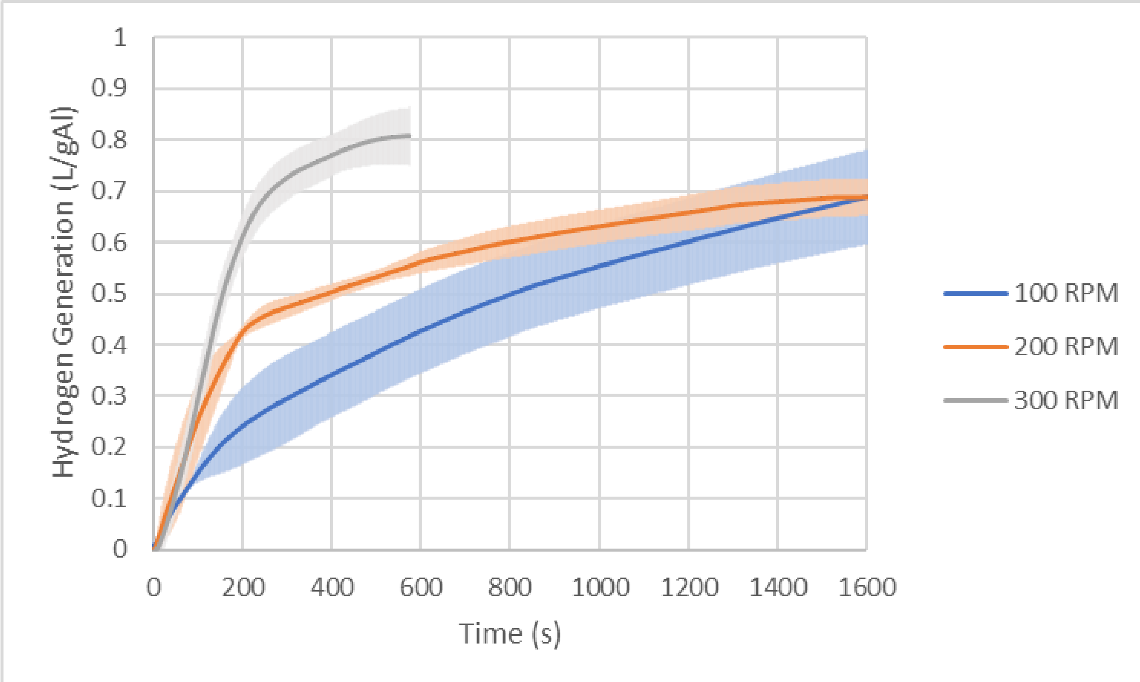

Figure 22: Integrated Hydrogen Production of Various Stirrer Spin Speeds. The lines represent the average integrated hydrogen generation profile of each test. The shaded regions depict the standard deviation of the test samples.

3.8.4 Impact of Parameters on Reaction Kinetics

Each parameter tested had an impact on the progression of the aluminum reaction. The temperature of the reaction had a significant impact on the peak reaction rate and the amount of hydrogen produced. The spin speed of the stirrer had the biggest impact on the total reaction time due to the turbulence diminishing the mass transport limitations of the particles through the slurry. Changes in the particle size had a significant effect on both peak reaction rate and the reaction time, likely due to the enhanced difficulty for the water to access smaller particles. To maximize the hydrogen production and decrease the amount of time it takes for the reaction to occur, the slurry should have larger particles and the reactor should be run at high temperatures and vigorously stirred.

4. ALUMINUM-SLURRY POWERED COOKING SYSTEM

4.1 Introduction to Cooking System

The second goal of the thesis was to develop a 500 W prototype cooking system that used the aluminum slurry to heat a water bath. For this to be accomplished, the system would need to be able to dispense the aluminum slurry into a reactor, contain hydrogen at low pressure, and safely combust the hydrogen. This section will cover the development of the cooking system concept, the operation of each of the major subsystems, and the results from the prototyping effort.

4.2 Review of Military Field Cooking

Military field cooking refers to the delivery, storage, and preparation of food for military personnel in operational environments. This field encompasses a large variety of missions from supporting individual soldiers to supplying battalion sized elements of hundreds of personnel.

4.2.1 Military Food Packaging Forms

The modern US military uses Meals-Ready-to-Eat (MREs) and Unitized Group Rations (UGR) as the fundamental packed food forms (Barrett, 2012). The MRE is a precooked individual meal that contains the basic nutrition needed for a typical soldier for moderate activity (Barrett, 2012). While no cooking is necessary, MREs contain a magnesium warming pouch that produces heat when water is added and can heat the food. The UGR-Heat and Serve system consists of precooked and shelf-stable rations that provide nutrition to up to 50 personnel when no refrigeration is available (Barrett, 2012). The UGR-Heat and Serve rations use either magnesium pouches like MRE heaters or use separate cooking equipment.

4.2.2 Modern Military Cooking Equipment

The main deployed equipment for military field cooking for unitized ration preparation is the Assault Kitchen. The Assault Kitchen contains the necessary equipment to warm UGR-Heat and Serve rations and can be packed into the bed of a HUMVEE (Barrett, 2021). The primary heater used in Assault Kitchens is the Tray Ration Heater System (TRHS) which can be seen in Figure 23.

Figure 23: Tray Ration Heater System (Babington, 2006)

The TRHS is a cooking device that uses a JP-8 burner and a heat exchanger to heat a water bath (Babington, 2006). UGR-Heat and Serve packs are submerged in the water bath to warm the rations for serving to personnel. The cooking system prototype developed for this thesis uses the same technique of heating a water bath for heating the rations. The main difference between the two heating devices is the way they heat the water bath. Instead of using a JP-8 burner, the system has an integrated aluminum reactor that transfers heat to the water bath and a hydrogen burner.

4.3 System Concept and Model

The prototype concept is based on the design of the Babington Tray Ration Heater System and is designed to heat a water bath using the aluminum-water reaction and heat from burning hydrogen. The aluminum slurry is pumped from a reservoir into the reactor and heats the water bath as seen in Figure 24. When the reactor is heated, it transfers heat into the surrounding water. The water in the reactor is separate from the water in the surrounding bath which prevents aluminum hydroxide and mineral oil from contaminating the food. The hydrogen generated in the reactor is diverted to a combustion system located under the water bath which transfers additional heat to the water.

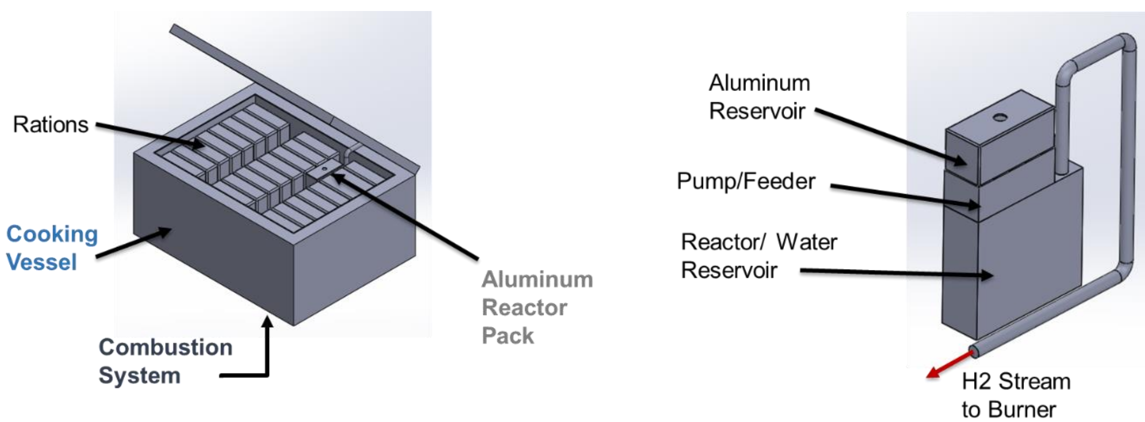

Figure 24: Concept of Cooking System

A model of an aluminum slurry powered system was created in COMSOL as seen in Figure 25. The purpose of the model is to predict the performance of the system and to determine if the concept was viable. The model is a 2-D representation of the system and uses the non-isothermal flow and reaction kinetics modules. The study was a time dependent study with a time step of 1 second. The model has a depth of 1 m and assumes no heat loss through the front or back of the system. The initial temperature of the model is 303 K. The insulation material is acrylic plastic. The temperature of the air surrounding the insulation layer is 300 K and a convective heat loss is used. The bottom of the vessel is assumed to be insulated Aluminum is fed into the reactor at a constant rate of 0.3 grams per second. There is no aluminum present in the reactor at the beginning of the simulation. The initial and boundary conditions can be seen below.

$$T = 303\ \mathrm{K}, t = 0 \text{ (Eq 4.1)}$$

$$Al = 0\ \mathrm{g}, t = 0 \text{ (Eq 4.2)}$$

$$dT/_{dx} = 10(T - 300),\ x = 0 \text{ (Eq 4.3)}$$

$$dT/_{dx} = 10(T - 300),\ x = 0.6 \text{ (Eq 4.4)}$$

$$dT/_{dy} = 0, y = 0 \text{ (Eq 4.5)}$$

$$dT/_{dy} = 10(T - 300), y = 0.6 \text{ (Eq 4.6)}$$

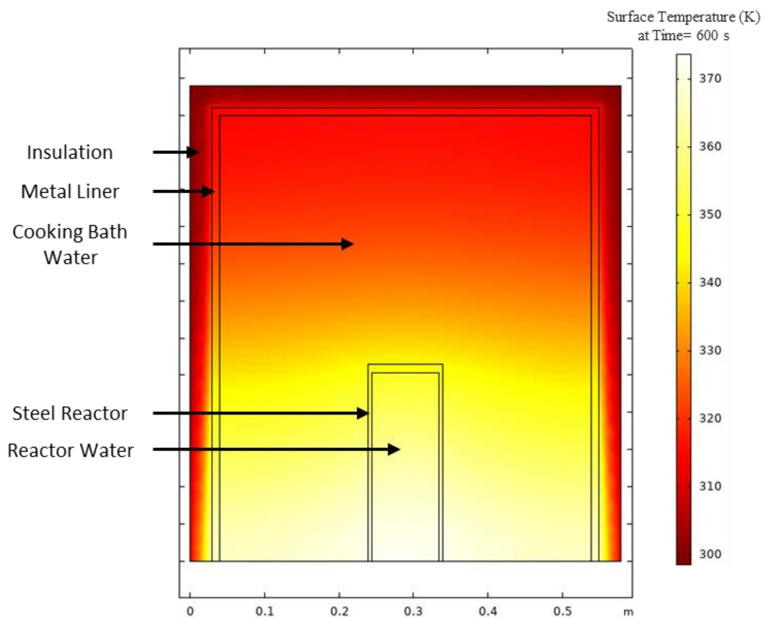

Figure 25: 2-D COMSOL Model

The model uses the Arrhenius equation to calculate the reaction rate of the aluminum in the reactor. The Arrhenius equation defines a rate constant K based on a pre-exponential frequency A and an exponential term

$$K = A * \exp\left({}^{-E}/_{RT}\right) \text{ (Eq 4.7)}$$

that uses the ideal gas constant R and an activation energy E in relation to the environmental temperature (Laidler, 1984). A preexponential factor of $7.24 \times 10^{8}\ \frac{1}{s}$ and an activation energy of $85{,}000\ \frac{J}{mol}$ was used to model the aluminum reaction rate. The rate constant is used to relate the consumption rate of the reactant dN/dt to the amount of reactant N present.

$$ {}^{dN}/_{dt} = K \times N \text{ (Eq 4.8)}$$

Heat is generated in the reactor water corresponding to the amount of aluminum consumed in that second. A heat flux is present at the bottom of the reactor to represent the heat addition by the combustion of the hydrogen. The hydrogen that is generated by the reaction is assumed to be immediately combusted with a heat exchanger efficiency of 80%. When the temperature in the reactor exceeds 90°C, no more aluminum is fed into the reactor until the reactor cools to 80°C. When the reactor temperature cools to 80°C more aluminum would be added until the reactor temperature reaches 90°C. This input scheme is implemented in the COMSOL model through the use of a temperature probe and the events module which changes the state of the aluminum feed pump between on and off states based on the temperature of the water in the reactor. This control scheme ensures that the water temperature in the reactor did not significantly overshoot and approach 100°C. The system continues to cycle the reactor temperature between 80 and 90°C until the bulk temperature of the surrounding water bath reaches 70°C.

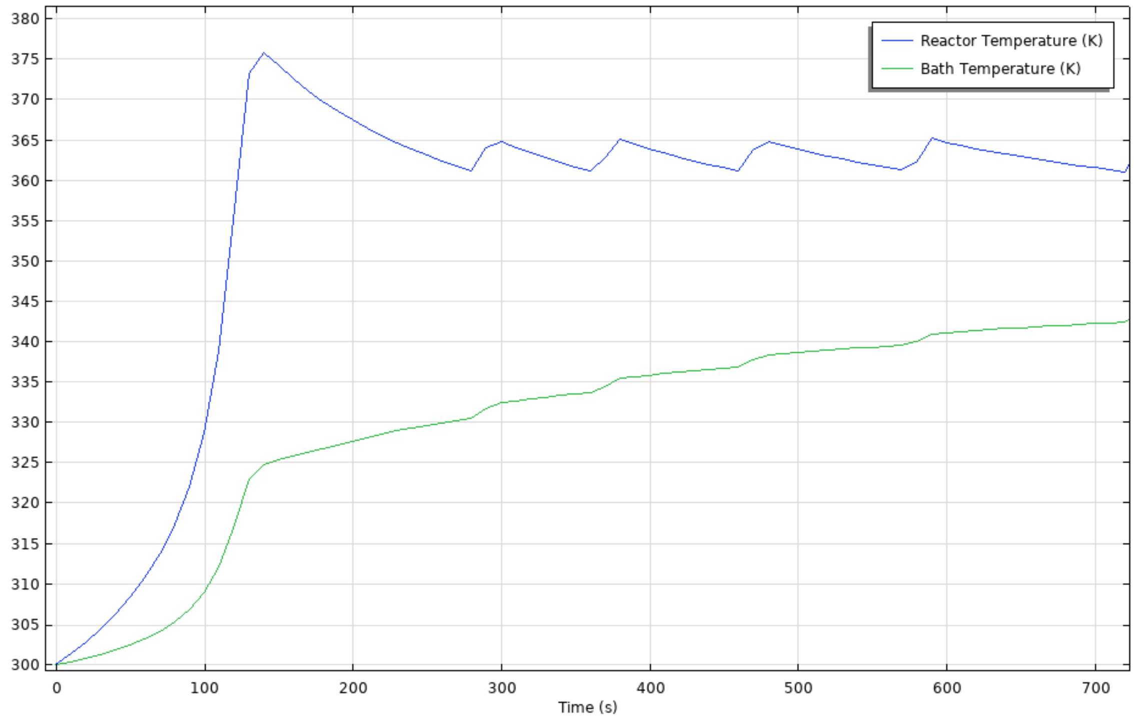

Figure 26: Average Water Temperature Profile from COMSOL Model

It was determined that the system would be the most unstable when it approached 40°C because of the presence of a large amount of unreacted aluminum as seen in Figure 26. The aluminum in the reactor takes 22 minutes to completely react at 30°C as found in experiments in Chapter 3. At higher temperatures, the reaction rate is so high that most of the aluminum would be consumed in seconds resulting in a system that is easier to control because the reaction delay is significantly shorter.

4.4 System Prototype

The system prototype cooking system consists of five subsystems: aluminum reactor, hydrogen manifold, combustion system, slurry dispenser and control system.

These subsystems slowly dispense aluminum, manage the flow of hydrogen, and enable heat transfer to a water bath. The completed prototype can be seen in Figure 27.

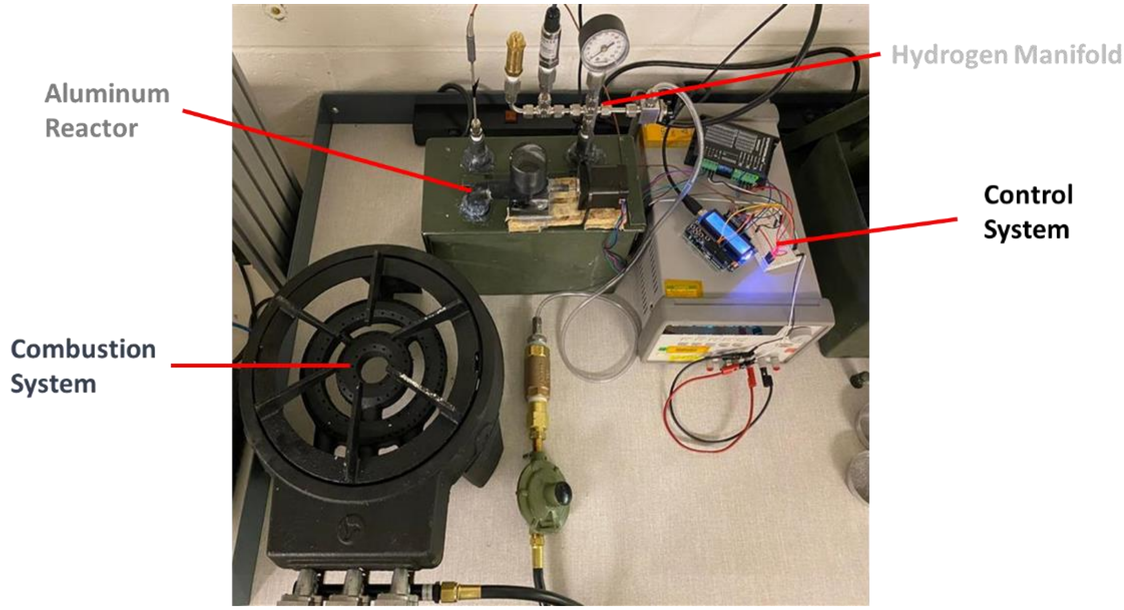

Figure 27: Cooking System Prototype without Cooking Vessel

4.4.1 Aluminum Reactor

The aluminum reactor is constructed from a modified M13 ammo can and through-wall bulk fittings and can be seen in Figure 28. The M13 ammo can was chosen because of the container's rectangular form factor, volume (approximately 6 liters), steel construction, non-sparking coating, and an airtight lid that could be opened. Three holes are drilled through the lid to enable through wall bulk fittings with ¼" NPT fittings to interface with the reactor as seen in Figure 28. An insulated type-k thermocouple is fitted to the reactor to measure the temperature of the water in the reactor. Dow Corning-3145 DC clear sealant was used to cover the holes and is found to be effective at holding hydrogen at low pressures once cured.

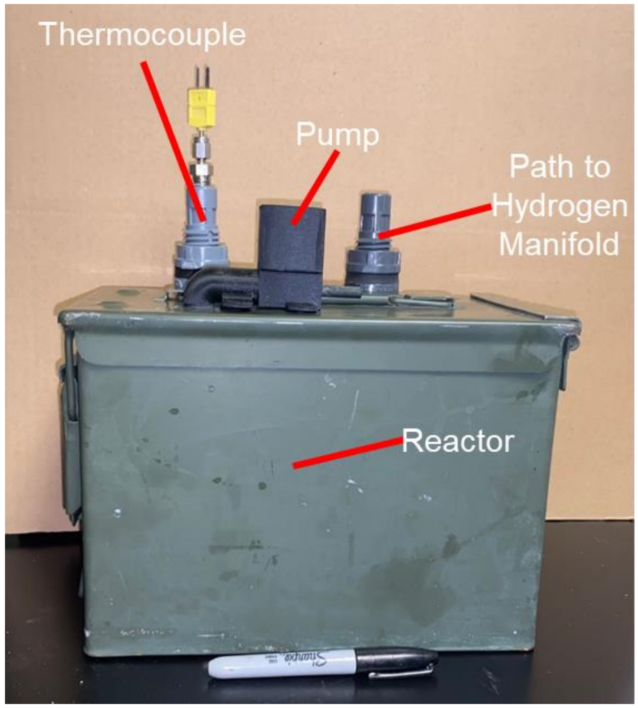

Figure 28: Prototype Reactor

4.4.2 Hydrogen Manifold

The hydrogen manifold is constructed out of ¼" steel Swagelok tubing and contains a pressure gauge, a digital pressure gauge, an automatic pressure relief valve, a manual relief valve, a check valve, and a bypass to the aluminum slurry container as seen in Figure 29. The purpose of the hydrogen manifold is to monitor and regulate the pressure of the reactor and to direct hydrogen to the combustion system while minimizing the hydrogen loss to the environment.

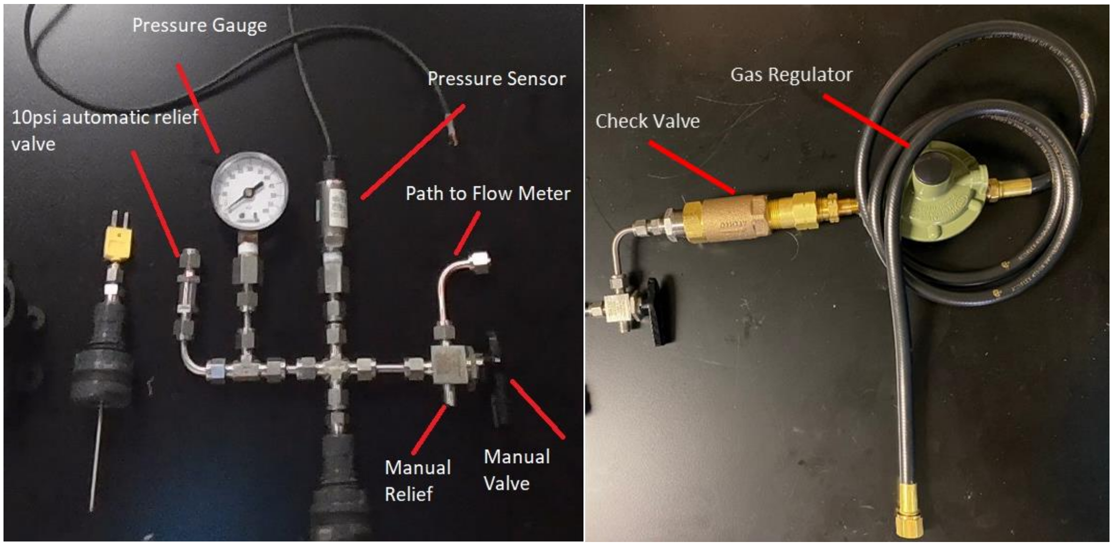

Figure 29: Hydrogen Manifold

The automatic pressure relief valve is set to release hydrogen once pressure exceeds 10 psi to prevent damage to the plastic components of the system. The check valve has a cracking pressure of 0.5 psi and sends hydrogen to the combustion system once the reactor pressure exceeds the limit. The purpose of the check valve is to enable one-directional flow of hydrogen and prevent oxygen or a flame from propagating back to the reactor.

4.4.3 Combustion System

The combustion system consists of three variable nozzles and a perforated tube as seen in Figure 30. The hydrogen gas mixes with the environmental air after passing through the nozzles which produces conditions favorable to combustion. The heat from the combustion transfers into the water bath through contact between the flames and the bottom of the water bath.

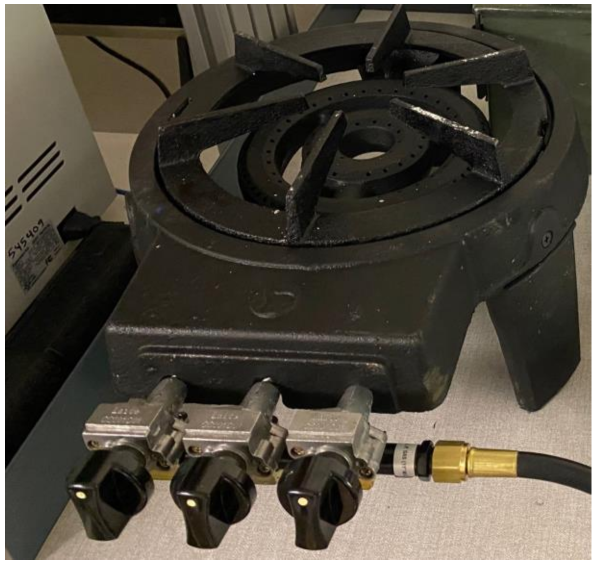

Figure 30: Combustion System

4.4.4 Slurry Dispenser

The slurry dispenser contains a 3D-printed screw pump, an aluminum slurry reservoir, and a stepper motor as seen in Figure 31. As discussed in Chapter 3, the screw pump was chosen during the aluminum slurry testing phase because it had low shearing of the fluid and the ability to dispense aluminum without clogging. When the stepper motor actuates the auger in the screw pump, the pump guides the aluminum slurry towards the outlet where it falls into the reactor. The pump relies on gravity to feed the aluminum from the reservoir into the auger. The viscosity of the aluminum slurry is a major factor in the ability to feed the aluminum from the reservoir because the pump is not able to pull a vacuum. If the viscosity is too high, the aluminum slurry cannot flow into the port on the bottom of the reservoir, enter the auger, and cannot be able to be guided by the auger into the reactor. The screw pump is not self-sealing, so there is a direct path leading from the reactor to the aluminum reservoir. The aluminum reservoir is pressurized to overcome the issue.

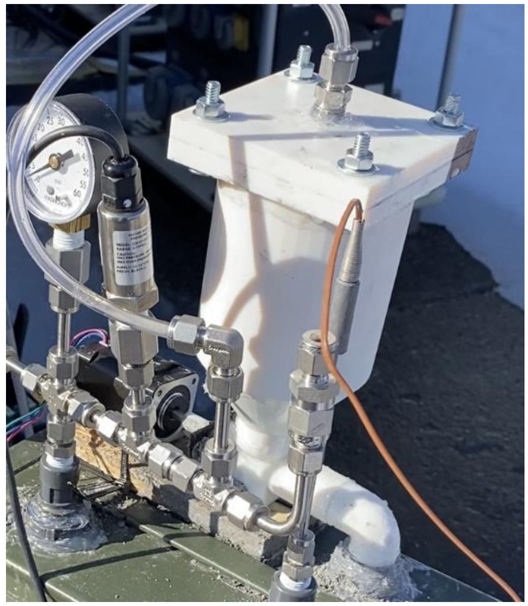

Figure 31: Aluminum Slurry Screw Pump

4.4.5 Slurry Dispenser Prototyping and Development

To create the final slurry dispenser seen in the previous subsection, multiple iterations of screw pumps were developed to address issues that arose during the prototyping effort as seen in Figure 32. The first screw pump was created for the slurry pumping tests covered in Chapter 3 to evaluate the ability for a screw pump to transport slurry. The second screw pump included a small aluminum slurry reservoir and a backing to prevent the rotor from moving along the length of the pump. The third screw pump included a larger aluminum reservoir, a bulkhead fitting to interface with the reactor, and a keyhole in the back of the rotor to enable a stepper motor to rotate the shaft. The fourth screw pump included a larger aluminum reservoir that was pressurized to prevent hydrogen from leaking through the top of the reservoir, and a thicker rotor to prevent the shaft from breaking.

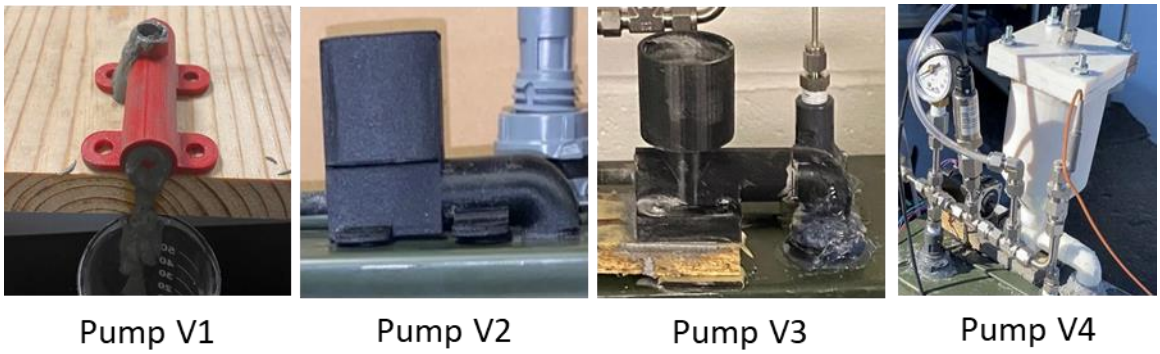

Figure 32: Screw Pump Prototype Iterations

4.4.6 Control System

The control system consists of an Arduino Rev 3, a stepper motor controller, and a variable power supply running at 24V seen below in Figure 33. The Arduino is fitted with an LCD touchscreen with buttons, a digital pressure sensor, and a thermocouple as inputs. To run the cooking cycle, the control system is activated and receives data from the thermocouple and pressure sensor. The system controls the aluminum dispense rate by varying the rotation of the stepper motor. An operator can also manually start and stop the dispensing of aluminum by using the buttons on the LCD screen.

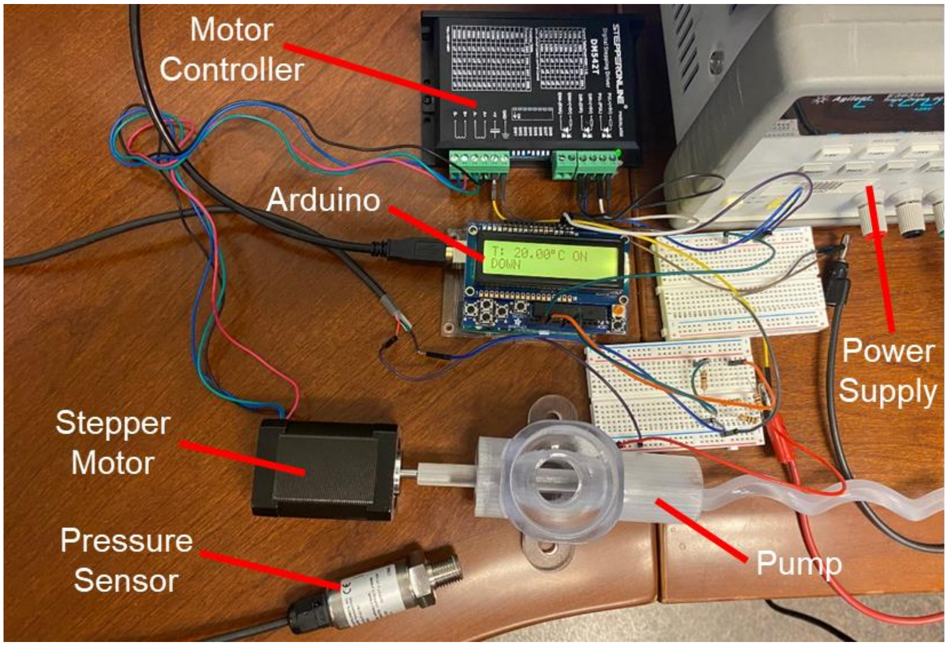

Figure 33: Control System

The control system tracks the approximate amount of aluminum dispensed into the reactor and uses the temperature and pressure data to predict how much aluminum is currently in the reactor and how much has been consumed. There is a significant delay between when the aluminum is dispensed into the reactor and when it reacts with the water as discussed in Chapter 3. The time delay is a function of the current reaction temperature and the thickness of the oil and aluminum layer on the water surface. As the temperature of the reactor increases, the reaction time greatly decreases as seen in Chapter 3. As more oil builds up on the surface, the time delay increases. The resulting balance results in a significant amount of unreacted aluminum acquiring in the reactor that quickly reacts when the water temperature exceeds 40℃. The feed rate of the aluminum is reduced between 35 and 50℃ to minimize the instability of the system. After the initial heating period the reaction rate of the aluminum exceeds the feed rate of the reactor resulting in a stable system that is easier to control. The system also pauses the motor if the pressure exceeds 5 psi or if the reactor reaches the desired temperature of 90 C to ensure the system does not over-pressurize or boil the water in the reactor.

4.5 Prototype Testing

4.5.1 Heat Transfer Testing

The goal of the heat transfer testing is to demonstrate the ability to controllably dispense aluminum slurry and heat 7 liters of water using the heat from aluminum-water reaction. The aluminum reservoir is filled with 300 ml of activated aluminum slurry (240 g of activated aluminum) and the reactor is filled with 4 l of water. The initial temperature of the water in the reactor is 18°C and the top of the insulating container is open to the environmental air at 8°C. The temperature of the water bath is monitored by a temperature sensor placed at the center of the insulating vessel. The experimental setup can be seen in Figure 34.

Figure 34: Prototype Testing Setup

To begin the test, the pump is activated and begins to dispense aluminum into the reactor. The temperature and pressure of the reactor are monitored to ensure that the reaction is controlled and does not experience over-pressurization. The hydrogen is sent to the combustion system and initially allowed to dissipate into the environment. When the temperature of the reactor reaches 35℃, the hydrogen combustion is initiated, and the flame is used to heat a separate body of water. The system continues to run until the aluminum slurry in the reservoir is consumed and all the hydrogen is consumed from the reactor.

4.5.2 Hydrogen Combustion Testing

The second part of testing the prototype is to safely ignite and maintain a flame with a stream of generated hydrogen. The valves in the combustion system are opened during the beginning of the testing to purge any air from the reactor. Hydrogen combustion is attempted when the reactor temperature reaches 35℃. To initiate the combustion, the valves are opened, and a grill sparker is used to generate a spark and initiate combustion. The flame is monitored to ensure that it is maintained and controlled. A FLIR thermal camera is used to observe the flame and measure the temperature of the surrounding area.

4.6 Cooking System Prototype Results and Discussion

The reactor was run for 125 minutes, and the combustion system was run for approximately 65 minutes. The system functioned properly, but there was significant heat loss to the environment due to the testing setup and the inability to close the lid of the insulating container.

4.6.1 System Function Results

The pump successfully dispensed approximately 95% of the aluminum. Some aluminum slurry was left on the surface of the hopper because the slurry was unable to feed itself back into the pump as seen in Figure 35. There was some minor leaking of the slurry out of the back of the pump rotor during the latter parts of the experiment, but this leaking did not cause the pump to jam or cease function. The reactor was able to manage and contain the hydrogen at 0.5 psi without leaking and was able to successfully direct hydrogen through the check valve and into the combustion system.

Figure 35: Aluminum Left in Reactor (left) and Leaking of the Pump (right)

4.6.2 Water Bath Heating Results

The reactor was unable to reach the goal temperature of 70℃ and reached a maximum temperature at 44℃. The water bath temperature reached 36℃ by the conclusion of the test. The full temperature changes can be seen in Table 6. The desired temperature was reached during previous indoor testing when the reactor was not submerged in a water bath. It is likely that the increased heat transfer from the reactor to surroundings caused the temperature to not rise as quickly.

Table 6: Thermal Results from Prototype Testing

Location	Starting Temperature (°C)	Peak Bulk Temperature (°C)	Temperature Difference
Reactor	20.48	44.14	23.66
Water Bath	17.56	36.00	18.44
Ambient Air	8	-	-

After the start of the test, it took 20 minutes for the temperature of the bath to start increasing as seen in Figure 36. The slow initial temperature rise rate was caused by the slow aluminum reaction rate at low temperatures. At 60 minutes, the temperature in the reactor reached 35°C, so the pump reduced the slurry feed rate. The temperature continued to constantly rise until the aluminum was fully consumed.

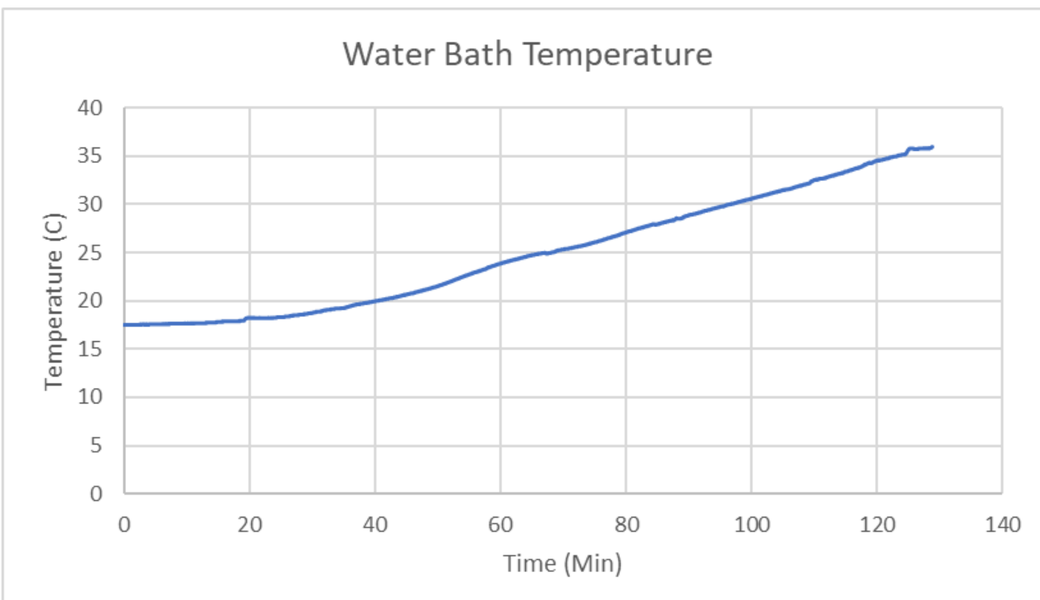

Figure 36: Temperature Profile at the Center of the Water Bath

The effectiveness of the heating system is determined by the ability to transfer heat from the aluminum reaction into the cooking bath. Due to the system design, the aluminum must heat the reactor water, fuel, and reactor in addition to the cooking bath.

The thermal energy results can be seen in Table 7. Due to the low temperature in the reactor throughout the course of the testing, only 30% of the activated aluminum dispensed into the reactor is expected to react with the water according to the results in Chapter 3. It was calculated that 36% of the heat generated was used to heat the reactor water, the reactor walls, and the reaction products. Additionally, 16% of the heat generated was lost to the environment through natural convection and evaporation, so only 14% of the energy from the aluminum fuel went into the water bath. The effectiveness of the system could be significantly improved by sealing the cooking vessel, increasing the ratio of cooking bath to reactor volume, and increasing the efficiency of the reaction.

Table 7: Thermal Energy Results of Heat Transfer Testing

	Thermal Energy (kJ)	Average Power (W)
Aluminum Input (240g)	3820	530
Estimated Reaction Efficiency	30%	
Reaction Thermal Energy	1150	160
Reactor Water/ Reaction Products	420	58
Heat Loss	190	26
Cooking Bath Water	540	75

4.6.3 Hydrogen Combustion Results

Once the reactor temperature reached 35℃, one of the valves to the combustion system was opened and the hydrogen was ignited using the grill starter. A hydrogen flame was produced and began to heat the second vessel. The aluminum in the reactor continued to produce hydrogen at a sufficient rate to crack the check valve and maintain the flame. The hydrogen flame was mostly invisible with only occasionally orange flickers to indicate that a flame was present. In the images in Figure 37, hydrogen is actively being combusted, but is not visible in the left image. The presence of carbon in the gas stream likely produces the orange color in the center image. The thermal image on the right indicates the temperature of the surrounding metal which is not hot enough to cause autoignition of hydrogen. The flame was maintained for 65 minutes and was manually extinguished when the test was completed.

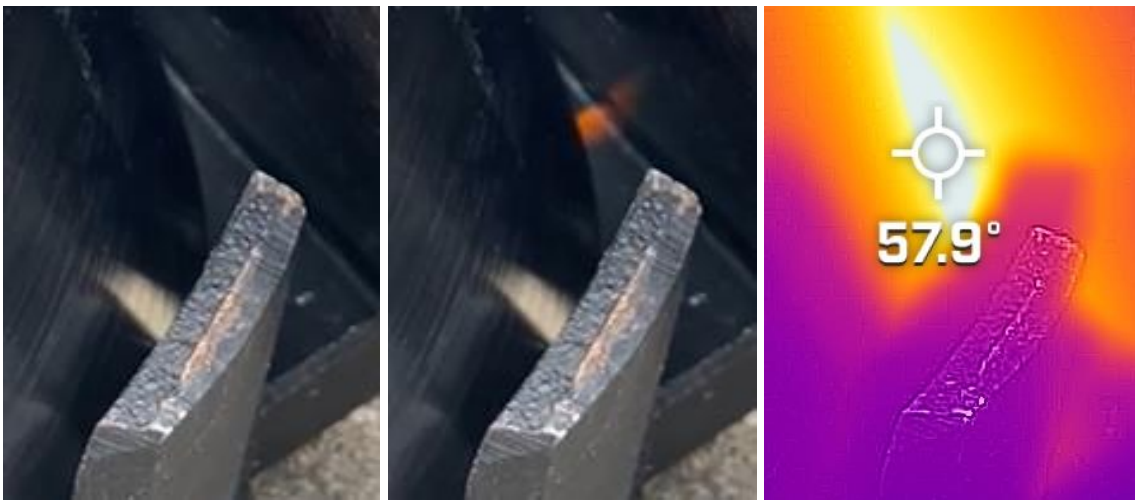

Figure 37: Lack of Consistent Color of Hydrogen Flame.

The flame was able to heat part of the metal cover that was closest to the center of the flame to approximately 142℃ as seen in Figure 38. The flame was able to transfer some heat to the water in the pot but was less effective at doing so as the distance from the flame was greater. The peak temperature in the water pot was 31℃ with the average temperature not exceeding 20℃. This lack of temperature rise can be attributed to the significant heat losses to the environment due to convective and radiative losses.

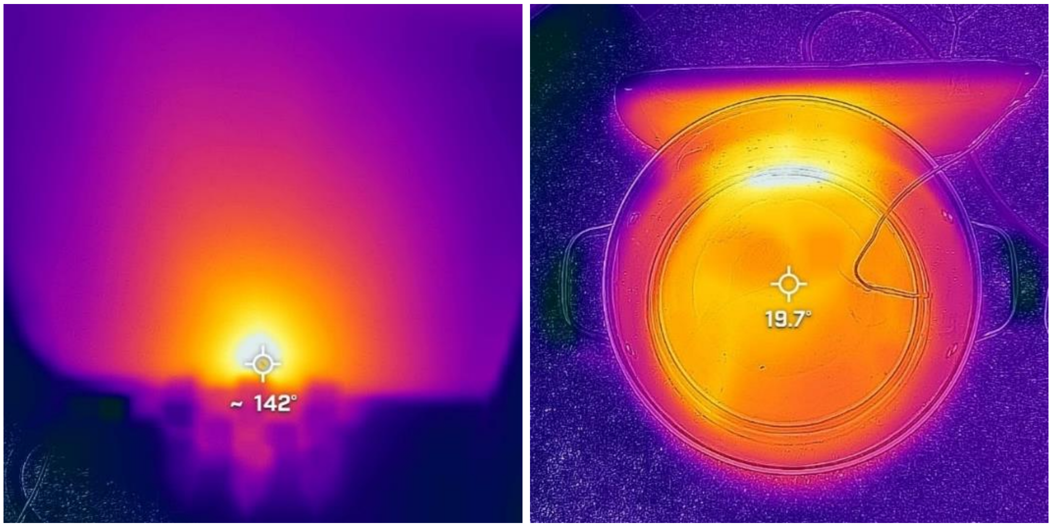

Figure 38: Heating of Cover and Water Vessel

5. CONCLUSIONS

5.1 Investigation into Slurry Transport and Reaction Kinetics

The properties of the activated aluminum slurry and the effect of additives on rheology were evaluated to determine the optimal mixture for pumping. It was found that reducing the mean particle size and the addition of 2 wt.% bentonite and 1 wt.% fumed silica created the optimal mixture for pumping applications. A review of pumping technologies was conducted, and two pumps were tested to identify possible methods for dispensing activated aluminum slurry. The screw pump was chosen for the cooking prototype due to the simplicity of the design and ability to pump the slurry with minimal jamming.

The effect of particle size, temperature, and stir speed on aluminum slurry reaction kinetics were also investigated. It was discovered that increasing the particle size and increasing the reactor water turbulence significantly decreased the reaction time and increased the power output. It was noted that the particle size and water turbulence dictated the ability for the aluminum to separate from the mineral oil and react with the water.

5.2 Cooking System Prototype

A prototype cooking system was developed that dispenses aluminum to heat a water bath and directs hydrogen to a combustion system. The system demonstrated a useful application for the heat generated by the aluminum-water reaction by heating up a water bath from 10 to 36°C in 8°C ambient conditions. While the system had a low fuel efficiency due to losses to the environment and low operating temperatures, the system could be improved to transport more heat into the cooking medium by having a larger cooking bath, and with a properly insulated and sealed container. The system affirmed the concept of using aluminum fuel to maintain a hydrogen flame at low pressure. The flame was found to be mostly colorless and was able to heat a pan to 142℃. The system offers a proof of concept for the application of aluminum slurry to provide productive heat energy and maintain a constant hydrogen stream and could be expanded into a more effective system with continuous improvement.

5.3 Future Research

The aluminum-slurry fuel is still in early development and will need additional improvement to become a fieldable fuel type. Future work includes the further testing of additives to improve the reaction efficiency, reduce the viscosity of the slurry at higher aluminum weight percentages, and introduce color to the hydrogen flame. Other future research includes evaluating different pumping technologies such as progressive cavity and pistons pumps due to their use in transporting other slurries. These pump types were not tested due to the complexity of their designs but may be promising due to possessing characteristics more suitable for pressurized systems and handling slurries with a high solid content. Additional testing on the slurry reaction kinetics in response to temperature should also be completed to improve the resolution of the results.

Additional research includes redesigning the cooking system prototype to increase the efficiency of transferring the energy from the aluminum to the water bath. The redesign includes integrating the hydrogen combustion system with the main system to provide heat to the water bath. Other improvements include the construction of a better insulation container and a better pressure vessel that can maintain higher pressures. If the system can operate at pressures from 30-50 psi, it would be able to build up a small hydrogen reservoir. The reservoir would permit the use of a flow controller and reduce the dependence of the hydrogen flame on the reaction rate of the aluminum.

BIBLIOGRAPHY

Babington, R. S. (2006). U.S. Patent No. 7,100,599. Washington, DC: U.S. Patent and Trademark Office.

Barrett, A. H., & Cardello, A. V. (2012). Military food engineering and ration technology. DEStech Publications, Inc.

Belcher, O., Bigger, P., Neimark, B., & Kennelly, C. (2020). Hidden carbon costs of the "everywhere war": Logistics, geopolitical ecology, and the carbon boot-print of the US military. Transactions of the Institute of British Geographers, 45(1), 65-80.

Chhabra, R. P. (2010). Non-Newtonian fluids: an introduction. In *Rheology of complex fluids* (pp. 3-34). Springer, New York, NY.

Choate, W. T., & Green, J. A. (2003). *US energy requirements for aluminum production: historical perspective, theoretical limits and new opportunities*. US Department of Energy, Energy Efficiency and Renewable Energy. https://www.energy.gov/eere/amo/downloads/us-energy-requirements-aluminum-production

COMSOL. (2021) "COMSOL Multiphysics Documentation." *COMSOL Multiphysics*

Crawford, N. C. (2019). Pentagon fuel use, climate change, and the costs of war. Watson Institute, Brown University. https://watson.brown.edu/costsofwar/files/cow/imce/papers/Pentagon%20Fuel%20Use%2C%20Climate%20Change%20and%20the%20Costs%20of%20War%20Revised%20November%202019%20Crawford.pdf

Department of the Army Headquarters, TM 10-7360-226-13&P. https://quartermaster.army.mil/jccoe/operations_directorate/fed/ck_manual.pdf

Eady, D. S., Siegel, S. B., Bell, R. S., & Dicke, S. H. (2009). *Sustain the mission project: Casualty factors for fuel and water resupply convoys*. CONCURRENT TECHNOLOGIES CORP JOHNSTOWN PA. https://apps.dtic.mil/sti/pdfs/ADB356341.pdf

Feys, D., De Schutter, G., Fataei, S., Martys, N. S., & Mechtcherine, V. (2022). Pumping of concrete: Understanding a common placement method with lots of challenges. Cement and Concrete Research, 154, 106720.

Fischman, J., Godart, P., & Hart, D. (2020). Hydrogen generation via the reaction of an activated aluminum slurry with water. International Journal of Hydrogen Energy, 45(35), 17118-17130.

Fraunhofer IFAM. (2013). Power on Demand by MgH2 Hydrolysis. https://www.ifam.fraunhofer.de/content/dam/ifam/en/documents/dd/Infobl%C3%A4tter/Power_on_demand_by_MgH2_hydrolysis_fraunhofer_ifam_dresden.pdf

Godart, P., Fischman, J., Seto, K., & Hart, D. (2019). Hydrogen production from aluminum-water reactions subject to varied pressures and temperatures. International Journal of Hydrogen Energy, 44(23), 11448-11458.

International Aluminum. (2022) Primary Aluminum Production.

Kaushal, D. R., Sato, K., Toyota, T., Funatsu, K., & Tomita, Y. (2005). Effect of particle size distribution on pressure drop and concentration profile in pipeline flow of highly concentrated slurry. International Journal of Multiphase Flow, 31(7), 809-823.

Laidler, K. J. (1984). The development of the Arrhenius equation. Journal of Chemical Education, 61(6), 494.

Morgan, E. R. (2018). Fuel Production Systems for Remote Areas via an Aluminum Energy Vector. Energy & Fuels, 32(9), 9033-9042.

Slocum, J. T. (2017). Characterization and science of an aluminum fuel treatment process (Doctoral dissertation, Massachusetts Institute of Technology). https://dspace.mit.edu/handle/1721.1/115674

Vlasak, P., & Chara, Z. (2011). Effect of particle size distribution and concentration on flow behavior of dense slurries. Particulate Science and Technology, 29(1), 53-65.

Weir, D. G. (1996). Strategic Implications for a Single-Fuel Concept. ARMY WAR COLL CARLISLE BARRACKS PA. https://archive.org/details/DTIC_ADA308981

Züttel, A. (2004). Hydrogen storage methods. Naturwissenschaften, 91(4), 157-172.

CURRICULUM VITAE

[redacted]

[redacted]